

**Rebuilding the Cepheid Distance Scale I:  
A Global Analysis of Cepheid Mean Magnitudes**

C.S. Kochanek

Harvard-Smithsonian Center for Astrophysics, MS-51

60 Garden Street

Cambridge MA 02138

Received \_\_\_\_\_; accepted \_\_\_\_\_

## ABSTRACT

We develop a statistical method for using multicolor photometry to determine distances using Cepheid variables including the effects of temperature, extinction, and metallicity and apply it to UBVRIJHK photometry of 694 Cepheids in 17 galaxies. We derive homogeneous distance, extinction and uncertainty estimates for four models, starting from the standard extragalactic method and then adding the physical effects of temperature distributions, extinction distributions, requiring positive definite extinctions, and metallicity. While we find general agreement with published distances when we make similar systematic assumptions, there is a clear problem in the standard distances because they require Cepheids with negative extinctions, particularly in low metallicity galaxies, unless the mean LMC extinction exceeds  $E(B - V) \gtrsim 0.25$ . The problem can be explained by the physically expected metallicity dependence of the Cepheid distance scale, where metal-poor Cepheids are hotter and fainter than metal-rich Cepheids. For V and I we found that the mean magnitude change is  $-0.14 \pm 0.14$  mag/dex and the mean color change is  $0.13 \pm 0.04$  mag/dex, with the change in color dominating the change in distance. The effect on Type Ia supernova estimates of the Hubble constant is dramatic because most were found in the metal poor galaxies with the bluest Cepheids. The Type Ia Multi-color Light Curve Shape (MLCS) method estimate for  $H_0$  formally rises from  $69 \pm 8$  km s<sup>-1</sup> Mpc<sup>-1</sup> to  $80 \pm 6$  km s<sup>-1</sup> Mpc<sup>-1</sup> with the metallicity correction.

*Subject headings:* Cepheids – distance scale – galaxies: distances and redshifts – Hubble Constant

## 1. Introduction

Cepheid variables are fundamental to most extragalactic distance estimates, determinations of the Hubble constant, and models for the structure of the Galaxy because the Cepheid period-luminosity (PL) relations are accepted as one of the most accurate primary distance indicators. In the last few years, the number of extragalactic Cepheids has exploded due to the two large extragalactic surveys using the Hubble Space Telescope (the Extragalactic Distance Scale Key Project (Freedman et al. 1994, Ferrarese et al. 1996, Graham et al. 1996, Kelson et al. 1996, Silbermann et al. 1996) and the Type Ia Supernova Calibration Project (Saha et al. 1994, 1995, 1996ab, 1997)), and the microlensing surveys of the Magellanic Clouds (e.g. Beaulieu et al. 1996, Welch et al. 1997). The goal of the HST projects is to determine the Hubble constant with 10% (0.2 mag) accuracy, which requires uncertainties in the Cepheid distance estimates, including all systematic uncertainties, that are still smaller. In order to reach these goals, the observational projects (see the review by Freedman 1997) have expanded the range of filters used to study Cepheids, particularly into the infrared, introduced systematic corrections for extinction, and tried to find good empirical tests for the effects of metallicity on Cepheid distance estimates.

The physical basis for Cepheids as distance estimators rests on two foundations (see the reviews by Feast & Walker (1987), Madore & Freedman (1991), and Tanvir (1996)). The first foundation is stellar structure, which closely correlates the mass, radius, luminosity, temperature, and oscillation period of a star, so that in any localized region of the H-R diagram there is period-luminosity-color (“PLC”) relation stating that the luminosity can be determined from the color (temperature) and the period (mass and radius) of oscillation. The second foundation is that the physics of the oscillations limits the Cepheids to a narrow range of luminosity and temperature called the instability strip. As a result, any projection of the three-dimensional PLC space onto a two-dimensional subspace produces a tightly

correlated relation. In particular, the period-luminosity (PL) correlations are defined by projecting over the temperature/color distribution. Both the PLC relations and the location of the instability strip are expected to be functions of composition (e.g. Stothers 1988, Stift 1990, Chiosi, Wood & Capitanio 1993), although there is great debate about the magnitude of the dependence and its measurement (e.g. Caldwell & Coulson (1986, 1987), Freedman & Madore (1990) Gould (1994), Stift (1995), Sasselov et al. (1996)). The sense, however, is that metal rich Cepheids are cooler and brighter than metal poor Cepheids at fixed period.

The goal of any analysis of Cepheid data is to accurately determine the distance to the Cepheid and its uncertainty, after compensating for the effects of period, temperature, composition, and extinction. Existing Cepheid analysis methods are divided into extragalactic and Galactic approaches. For extragalactic systems the analysis must determine the common distance of an ensemble of Cepheids, usually based on two-color, low-accuracy photometry, with poor phase coverage. The standard approach (see Madore & Freedman 1991) uses only the correlation between luminosity and period (the PL relations) to estimate the distance modulus and the mean extinction. Gould (1994) pointed out that the method is statistically inefficient because it ignores the strong correlations in the residuals (i.e. the PLC relations). Galactic analyses (e.g. Caldwell & Coulson 1986, 1987, Caldwell & Laney 1991, Laney & Stobie 1993, 1994) must estimate the distances and extinctions of individual Cepheids using three-color photometry and PLC relations because the Cepheids no longer lie at a common distance. The standard extragalactic approach explicitly ignores the PLC relations, and the standard Galactic approach (in some senses) ignores the instability strip.

In the following sections we develop a self-consistent physical and mathematical analysis of multi-color Cepheid mean magnitudes as the first in a series papers reanalyzing the Cepheid distance scale. Our approach differs from the standard approaches in three

major ways. The first difference is that we analyze all the data simultaneously rather than one galaxy at a time. The use of Cepheids as distance indicators is predicated on the homogeneity of their physical properties, so either all the data can be self-consistently and simultaneously analyzed or we must reject the Cepheids as distance indicators. Moreover, the distance estimates (and other physical parameters) are very highly correlated. Any change in the distance or extinction estimate for one Cepheid galaxy requires a simultaneous change in the values for all Cepheid galaxies. The second difference is that we avoid the false dichotomy between the Galactic and extragalactic analysis procedures, and demonstrate how to reconcile the two approaches. The resulting statistical method has greater statistical efficiency than traditional methods, can model all measured colors simultaneously, and allows for better control, treatment, and understanding of systematic problems such as individual Cepheid extinctions and the effects of metallicity. The resulting scheme, although based on a physical model, closely resembles the empirical treatments of Gould (1994) and Sasselov et al. (1996). The third difference is that we explore the important systematic errors that can affect the Cepheid distance estimates, particularly the physics of extinction, temperature and metallicity. While treatments of extragalactic Cepheid distances generally recognize the existence of these systematic uncertainties, they are rarely included in the distance estimates or their uncertainties. We develop our analysis method in §2, and compare it to the existing techniques. In §3 we examine the Cepheid correlations (PL, PLC relations etc.) and the resulting distance estimates. We summarize our results, their shortcomings, and possible solutions in §4.

## 2. Cepheid Distance Estimates

We assume that the bolometric luminosity and the bolometric correction are linear functions of the period  $p = \log P/P_0$ , the effective temperature  $t = \log T_e/T_0$ , and the

(logarithmic) metallicity  $Z$ , so that the (intensity mean) apparent magnitude  $V_k$  of a Cepheid in band  $k$ , at distance modulus  $\mu$ , with extinction  $E$  is

$$V_k = V_{0k} + \alpha_k p + \beta_k t + \gamma_k Z + \mu d_k + ER_k \quad (1)$$

where  $V_{0k}$  is the magnitude zero-point vector,  $R_k$  is the reddening vector,  $d_k \equiv 1$  is the distance vector, and  $\log P_0 = 1.4$  and  $T_0$  are reference periods and temperatures. We assume that the slopes  $\alpha_k$  and  $\beta_k$  are independent of metallicity, although theory predicts a weak dependence (see Stothers 1988, Stift 1990, 1995, Chiosi et al. 1993). If we neglect the dependence of bolometric corrections on surface gravity,  $\alpha_k = \alpha_j$ . We call eqn. (1) a period-luminosity-color (PLC) relation, although standard PLC relations (see Feast & Walker 1987) replace the effective temperature by a color. We neglect additional variables such as the Cepheid’s age, the instability strip crossing number, the helium abundance, and non-linearities in the PLC relation (see Caldwell & Coulson 1986), so we assume that the relations defined by eqn. (1) have an intrinsic width of  $\sigma_{PLCk}$ .

Formally, if we know the precise values of the vectors  $\alpha_k$ ,  $\beta_k$ ,  $\gamma_k$  and  $R_k$ , the vectors are not degenerate with  $d_k$  ( $\equiv$  distance), and we possess accurate photometry of the Cepheid in a sufficiently large number of bands, then the PLC relations can be used to determine the distance to a particular Cepheid. Unfortunately, since we must determine  $\alpha_k$ ,  $\beta_k$  and  $\gamma_k$  as we proceed from a small number of colors, it is difficult to use the PLC relations to determine distances without adding additional constraints. The additional constraints used in standard Cepheid analyses (e.g. Madore & Freedman 1991) correspond to adding priors on the distances and extinctions. We now develop a general mathematical description for fitting Cepheid magnitudes that includes the standard methods as subcases or limits of a more general model.

The PLC relations contain no information about which stars pulsate, and the most important prior information is the location and width of the instability strip. The

standard extragalactic method uses the instability strip by averaging the distribution over temperature and using only the PL relations to determine distances. We parametrize the instability strip by a period-color (PC) relation defining the temperature distribution for stars at a fixed period using a likelihood function

$$L(t|p) \propto \exp \left[ -\frac{(t - \delta_Z Z - \delta_P p)^2}{2\sigma_{PC}^2} \right] \quad (2)$$

including a possible shift in the location of the instability strip with metallicity (e.g. Stiff 1990, Chiosi et al. 1993). We assume that the width of the instability strip is constant, although the observed narrowing of the strip at short periods (e.g. Fernie 1990) could be modeled by making  $\sigma_{PC}$  a function of period (e.g. Gould 1994). We chose to parametrize the instability strip with a PC relation rather than a luminosity-color relation (i.e. the H-R diagram) because it is distance independent and uses the well-defined period as the independent variable instead of the luminosity. From these two assumptions we can derive all the standard relations used to study Cepheids and their correlations. For example, the PL relation in band  $V_k$  is

$$\frac{\int V_k L(t|p) dt}{\int L(t|p) dt} = \langle V_k \rangle = V_{0k} + \alpha'_k p + \gamma'_k \langle Z \rangle + \mu d_k + \langle E \rangle R_k \quad (3)$$

where  $\alpha'_k = \alpha_k + \beta_k \delta_P$  and  $\gamma'_k = \gamma_k + \beta_k \delta_Z$ , and the dispersion in the relation is  $\sigma_{PLCk}^2 + \beta_k^2 \sigma_{PC}^2 \simeq \beta_k^2 \sigma_{PC}^2$  since  $\sigma_{PLCk} \ll \sigma_{PC}$ . From here on we use the deviation of the temperature from the expected mean,  $\delta t = t - \delta_Z Z - \delta_P p$ , which also shifts the period and metallicity vectors to the  $\alpha'_k$  and  $\gamma'_k$  appearing in the PL relation (3). We cannot independently determine  $\alpha_k$ ,  $\gamma_k$ ,  $\delta_Z$  and  $\delta_P$  without absolute temperature references, so we restrict our solutions to determinations of  $\delta t$ ,  $\alpha'_k$ , and  $\gamma'_k$ . We measure distances, extinctions, and metallicities relative to the LMC values of  $\langle \mu \rangle_{LMC}$ ,  $\langle E \rangle_{LMC}$ , and  $Z_{LMC} \equiv [O/H]_{LMC}$ . We use the oxygen abundance for the metallicity variable because it is the only abundance available for most of the extragalactic systems. We can also constrain the models using prior information on the distance modulus, extinction, and metallicity. In external galaxies we

can use the constraint that all Cepheids lie at the same distance, but this assumption begins to fail for the LMC and may be a poor assumption for the SMC (e.g. Caldwell & Coulson 1986, Caldwell & Laney 1991). We allowed the Magellanic Clouds to be tilted relative to the line of sight, and to have a finite thickness. Distances and extinctions were fit for each Galactic Cepheid, constrained by the non-linear likelihood of fitting the measured radial velocity with a flat rotation curve. From the rotation curve model we obtain estimates of the solar radius  $R_0$  and circular velocity  $\Theta_0$ . We model the priors using Gaussians with mean values of  $\langle\mu\rangle$  for the distance modulus,  $\langle E\rangle$  for the extinction, and  $\langle Z\rangle$  for the metallicity, with dispersions of  $\sigma_\mu$ ,  $\sigma_E$ , and  $\sigma_Z$  for each galaxy or Cepheid. The relative calibration of the standard and the HST V and I magnitudes is uncertain at the level of 0.05 mag (Hughes et al. 1994), so we include two HST calibration variables constrained by a Gaussian prior of width 0.05 magnitudes in the likelihood. The temperature  $\sigma_{PC}$  and PLC  $\sigma_{PLCk}$  widths were the same for all galaxies.

We can divide our analysis into two parts. First, we estimate the parameters of the individual Cepheids ( $\mu$ ,  $\delta t$ ,  $E$ , and  $Z$ ) given the current parameters of the global model. Second, we optimize the parameters ( $V_{0k}$ ,  $\alpha'_k$ ,  $\beta_k$ ,  $\gamma'_k$ ,  $\dots$ ) of the global model. For a particular Cepheid we have mean magnitude measurements  $V_{mk}$  with uncertainties  $\sigma_{mk}$  in each of  $k = 1 \dots N$  bands and a known period  $P$ . If we define  $\sigma_k^2 = \sigma_{mk}^2 + \sigma_{PLCk}^2$ , then the log-likelihood for the model to fit the measured mean magnitudes  $V_{mk}$  of a particular Cepheid is

$$-2 \ln L = \sum_{k=1}^N \frac{(V_{mk} - V_k)^2}{\sigma_k^2} + \frac{\delta t^2}{\sigma_{PC}^2} + \frac{(E - \langle E \rangle)^2}{\sigma_E^2} + \frac{(\mu - \langle \mu \rangle)^2}{\sigma_\mu^2} + \frac{(Z - \langle Z \rangle)^2}{\sigma_Z^2} + \ln |S^{-1}| \quad (4)$$

up to a constant, where the covariance matrix is

$$S_{ij}^{-1} = \sigma_i^2 \delta_{ij} + \sigma_\mu^2 d_i d_j + \beta_i \beta_j \sigma_{PC}^2 + R_i R_j \sigma_E^2 + \gamma'_i \gamma'_j \sigma_Z^2, \quad (5)$$

and the indices run over the filters included in the calculation. We must use the determinant



of the covariance matrix  $S$  in the likelihood if we are to simultaneously determine the properties of the individual Cepheids and their global statistical relations.

We can relate our model to standard analyses by breaking the calculation into two sections: first, deriving the deviations in the properties of individual Cepheids from the mean, and second, determining the PLC relation vectors and the mean properties of the Cepheids. If we measure the magnitude residuals  $\Delta V_k = V_{mk} - \langle V_k \rangle$  relative to the mean PL relations (eqn. (3)) for the parent galaxy, define the deviation of the Cepheid parameters from the mean parameters by  $x$  and the vector-weighted residuals by  $v$ ,

$$x = \begin{pmatrix} \delta t \\ E - \langle E \rangle \\ \mu - \langle \mu \rangle \\ Z - \langle Z \rangle \end{pmatrix} \quad \text{and} \quad v = \begin{pmatrix} \sum_k \Delta V_k \beta_k / \sigma_k^2 \\ \sum_k \Delta V_k R_k / \sigma_k^2 \\ \sum_k \Delta V_k d_k / \sigma_k^2 \\ \sum_k \Delta V_k \gamma'_k / \sigma_k^2 \end{pmatrix}, \quad (6)$$

and define the matrix  $C$  by

$$C = \begin{pmatrix} \sum_k \frac{\beta_k^2}{\sigma_k^2} + \frac{1}{\sigma_{PC}^2} & \sum_k \frac{\beta_k R_k}{\sigma_k^2} & \sum_k \frac{\beta_k d_k}{\sigma_k^2} & \sum_k \frac{\beta_k \gamma'_k}{\sigma_k^2} \\ \sum_k \frac{\beta_k R_k}{\sigma_k^2} & \sum_k \frac{R_k^2}{\sigma_k^2} + \frac{1}{\sigma_E^2} & \sum_k \frac{R_k d_k}{\sigma_k^2} & \sum_k \frac{R_k \gamma'_k}{\sigma_k^2} \\ \sum_k \frac{\beta_k d_k}{\sigma_k^2} & \sum_k \frac{R_k d_k}{\sigma_k^2} & \sum_k \frac{d_k^2}{\sigma_k^2} + \frac{1}{\sigma_\mu^2} & \sum_k \frac{d_k \gamma'_k}{\sigma_k^2} \\ \sum_k \frac{\beta_k \gamma'_k}{\sigma_k^2} & \sum_k \frac{R_k \gamma'_k}{\sigma_k^2} & \sum_k \frac{d_k \gamma'_k}{\sigma_k^2} & \sum_k \frac{\gamma_k'^2}{\sigma_k^2} + \frac{1}{\sigma_Z^2} \end{pmatrix} \quad (7)$$

then  $x = C^{-1}v$  and the covariance matrix of the parameter estimates for a fixed PLC relation is  $C^{-1}$ . With the optimization of these variables, the contribution of the Cepheid to the likelihood becomes

$$L \propto |S|^{-1/2} \exp\left(-\frac{1}{2} \Delta V^T S \Delta V\right) \quad (8)$$

where  $\Delta V$  is the vector of residuals relative to the mean PL relations and  $S$  is the covariance matrix defined in eqn. (5).

We obtain the standard extragalactic method (see Madore & Freedman 1991) if the four priors have zero width ( $\sigma_{PC} = \sigma_E = \sigma_\mu = \sigma_Z = 0$ ) and there is no metallicity dependence

( $\gamma'_k = 0$ ). The covariance matrix  $S_{ij} = \delta_{ij}(\sigma_{mi}^2 + \sigma_{PLCi}^2)$  is diagonal. Some extragalactic Cepheid distances are derived by using reddening free distances or determining individual extinctions (e.g. Freedman et al. 1990, 1991, 1992, Tanvir et al. 1995, Saha et al. 1996ab, 1997), which corresponds to allowing  $\sigma_E \rightarrow \infty$ . If we optimize the widths of the priors, then the method matches that of Gould (1994) or Sasselov et al. (1996) in using the covariance matrix of the residuals to build a better statistical model of the data. The advantage of our formalism is that it derives from a physical model and we gain new physical insights into the system from the variables making up the covariance matrix. The disadvantage is that if our physical model is incorrect or it is missing important sources of correlated variance in the data, it is not as optimal or correct a statistical approach as using a purely empirical covariance matrix. If we limit the model to two or three filters and use broad priors we recreate the normal Galactic approach (e.g. Caldwell & Coulson 1986, 1987, Laney & Stobie 1986, 1993, 1994, Fernie 1990, Fernie et al. 1995) with the color dependence of the standard PLC relations appearing indirectly through the temperature variable.

Three classes of data and parameters enter the problem. The first class consists of the period and the composition. Here we know the dependent variable ( $p$  or  $Z$ ), and seek to determine the state vectors ( $\alpha'_k$  and  $\gamma'_k$ ). Given an adequate range for the dependent variables in an external galaxy, the state vectors are well-determined and non-degenerate. In particular, the standard PL relations (e.g. Madore & Freedman 1991, Laney & Stobie 1994, Tanvir 1996) determine  $\alpha'_k$  based on the Cepheids in the LMC. In the second class, consisting of the extinction and the distance, we know the state vectors ( $R_k$  and  $d_k$ ) and would like to determine the dependent variable ( $E$  and  $\mu$ ). The distance vector is known exactly ( $d_k \equiv 1$ ), and the extinction vector  $R_k$  is known approximately (see §2.2). With accurate measurements in a sufficient number of bands, we can determine the distances and extinctions for individual Cepheids. The uncertainties will depend on how well we can determine the effects of temperature and metallicity, but the formalism will correctly

include these uncertainties in the distance and extinction estimates.

In the third case, the temperature, we know neither the dependent variable  $t$  nor the state vector  $\beta_k$ . One immediate consequence is the existence of a mathematical degeneracy under a rescaling of the temperature by  $t \rightarrow \xi t$ . The likelihood is unchanged if we rescale the other temperature related variables by  $\beta_k \rightarrow \xi^{-1}\beta_k$ ,  $\delta_P \rightarrow \xi\delta_P$ ,  $\delta_Z \rightarrow \xi\delta_Z$  and  $\sigma_{PC} \rightarrow \xi\sigma_{PC}$ . No observable (i.e. magnitude) depends on the rescaling, and it means that we cannot set an absolute temperature scale. A more fundamental problem is that values found for variables such as the  $t$ - $\beta_k$  pair may not have physical meaning assigned to them in the mathematical model. The minimization procedure will simply use them to absorb as much variance as possible from the residuals, and if  $\beta_k$  is unconstrained it assumes the value of the most important unmodeled principal component of the true covariance matrix. Only if the primary source of the variance is the temperature distribution at fixed period will  $t$  represent the physical temperature. In essence, we are defining the covariance matrix in terms of a few principal components defined by the state vectors, and we assert that the  $\beta_k$  principal component represents temperature. The degeneracy only affects our interpretation of the variables, and the statistical model will still reproduce the correct observational PLC/PC/PL relations. For practical purposes we solved the degeneracy problem by using a prior for the  $\beta_k$  derived from fitting Cepheid light curves, which we discuss in paper II (Kochanek 1997b). The difficulty in estimating  $\beta_k$  (or its equivalent slope in standard PLC relations) and separating temperature from extinction has lead the extragalactic Cepheid community to avoid modeling the temperature distribution (e.g. see the critique of PLC relations in Madore & Freedman 1991).

## 2.1. Data

We simultaneously analyzed the Cepheids of 17 galaxies (see Table 1), including only Cepheids with periods between 7 days and 80 days. We used all available Johnson UBV, Kron-Cousins RI, and Glass-Carter JHK mean magnitudes for the Cepheids, because the systems with many color photometry (the Galaxy, LMC, SMC, M 31, M 33, and NGC 300) offer the best hope of separating the effects of distance, temperature, extinction, and metallicity. With two-color photometry there is no simple means of separating the effects of temperature and extinction, while with eight-color photometry it should be possible. We assigned magnitude uncertainties of 0.05 mag for the Galactic, LMC and SMC Cepheids, and 0.10 mag for the HST Cepheids and the poorly sampled ground-based data on M 31, M 33, and NGC 300. Estimates of the distances and extinctions were little affected by changes in the estimated measurement errors. Although we spot-checked many of the inferred magnitudes and periods for the Cepheids, we used the published periods and magnitudes in our analysis.

Galaxy: We used the Cepheids with radial velocities in Pont et al. (1994) and periods longer than 7 days. Intensity mean magnitudes were checked from the data compilations by Welch (1996) and Berdnikov (1987, 1996), and matched existing B and V tabulations (e.g. Fernie et al. 1995). We dropped the Cepheids AA Ser, XZ Car, and SU Cru from the Pont et al. (1994) sample as outliers.

LMC: We used the UBVI data from Caldwell (1996), the JHK data from Laney & Stobie (1986, 1993, 1994) which includes earlier data by Welch et al. (1987), and the R data from Madore (1985). The Caldwell (1996) mean magnitudes include earlier data whose sources are reviewed in Madore (1985). We rejected HV2301, HV2378 and HV2749 from our fits as outliers in the likelihood. Caldwell & Laney (1991) and earlier authors also report that these three Cepheids have abnormal properties.

SMC: We used the BVRI data from Caldwell (1996) and the JHK data from Laney & Stobie (1993, 1994). We rejected HV854, HV1369, HV1438, HV1482, HV1484, and HV1695 as outliers in the likelihood. Caldwell & Laney (1991) and earlier authors report HV1369, HV1484, HV1636, and HV1641 as outliers. We find nothing peculiar about HV1636, and HV1641 was not included in the sample from Caldwell (1996).

M 33: We use the BVRI data from Freedman, Wilson & Madore (1991) excluding 21979, 23764, and B1. The photometry for V12 in Table 5 of Freedman et al. (1991) is shifted to the left by one column. None of the remaining Cepheids stood out in the likelihood distribution.

M 31: We use the BVRI data from Freedman & Madore (1990, Freedman 1996). We rejected the 18.5 day period Cepheid in Baade’s Field III.

NGC 300: We use the BVRI data from Freedman et al. (1992). We rejected V21 as an outlier. Freedman et al. (1992) comment that the light curve of V21 is not well determined.

M 81: We use the VI data from Freedman et al. (1994). We left the magnitude calibrations unchanged. We rejected C8 as an outlier.

M 100: We use the VI data from Farrarese et al. (1996). There is a typographical error in the distance modulus given in the abstract of Farrarese et al. (1996, erratum 1997), where the correct value is  $\mu = 31.04 \pm 0.17$ . We added the 0.05 mag “long exposure correction” to the tabulated Cepheid magnitudes (Hughes et al. 1994). We rejected the two shortest period Cepheids, C68 and C70 as outliers.

M 101: We use the VI data from Kelson et al. (1996) including all the I photometry (the “weak photometry restriction”). The light curve data tables of Kelson et al. (1996)

have the time and magnitude columns in different orders. We rejected C28 as an outlier.

IC 4182: We use the VI data from Saha et al. (1994). We rejected C3-V9 as an outlier.

NGC 5253: We use the VI data from Saha et al. (1995). We rejected C3-V1 and C3-V2 as outliers.

NGC 4536: We use the VI data from Saha et al. (1996a). Following the authors we included only Cepheids with periods longer than 20 days and quality class 4-6 in the standard analysis. We added the 0.05 mag “long exposure correction” to the tabulated Cepheid magnitudes. We rejected C3-V12, C3-V16, C3-V24, and C3-V31 as outliers.

NGC 925: We use the VI data from Silberman et al. (1996). We rejected 3–11, 3–29, 4–68, and 4–71 as outliers.

M 96: We use the VI data from Tanvir et al. (1995).

NGC 3351: We use the VI data from Graham et al. (1996) but restricted our sample to periods longer than 10 days. We rejected C7, C17, C23, and C46 as outliers.

NGC 4496A: We use the VI data from Saha et al. (1996b). Following the authors we included only Cepheids with periods longer than 17 days and quality class 4-6 in the standard analysis. We added the 0.05 mag “long exposure correction” to the tabulated Cepheid magnitudes.

NGC 4639: We use the VI data from Saha et al. (1997). Following the authors we included only Cepheids with periods between 20 and 63 days and quality class 4-6 in the standard analysis. We added the 0.05 mag “long exposure correction” to the tabulated Cepheid magnitudes.

## 2.2. Extinction

We require an extinction vector  $R_k = A_k/E(B - V)$  defined for all eight filters. Our standard vector is  $R_{0k} = (5.05, 4.31, 3.30, 2.73, 2.07, 0.95, 0.64, 0.39)$  for the UBVRIJHK filters based on the Cardelli, Clayton & Mathis (1989) model for the extinction curve. We fixed  $R_V = 3.3$  to match the Key Project, but as emphasized by Cardelli et al. (1989) the difference between  $R_V = 3.1$  and  $R_V = 3.3$  is mainly in the absolute normalization of the  $R_k$  vector and the estimated  $E(B - V)$ . The shape of the extinction vector changes very little. The Type Ia project uses  $A_V/A_I = 1.7$  instead of  $A_V/A_I = 1.6$ . The earlier M 31 (Freedman & Madore 1990) and M 33 (Freedman et al. 1991) studies used  $R_V = 3.1$  combined with the Cardelli et al. (1989) extinction curve, while  $R_V = 3.3$  was used for NGC 300 (Freedman et al. 1992). Laney & Stobie (1993) estimated that the JHK values were (0.82, 0.49, 0.30). We do not include the temperature variations in the extinction coefficient used by many of the Galactic Cepheid models (e.g. Caldwell & Coulson 1986, Laney & Stobie 1986, 1993, 1994, Feast 1987, Fernie 1990).

Cepheid distances are sensitive to the assumed structure of the extinction vector  $R_k$ , but most existing treatments of Cepheid distances treat the extinction as a known, understood property of the ISM even while different analyses select different models. Exceptions are Laney & Stobie (1993, 1994) and Sasselov et al. (1996), who systematically varied the  $R_k$  or tried to determine them from the data, and Freedman et al. (1990, 1991) who examined the effects of using standard  $R_V = 3.1$  or 3.3 or extremal models on the distance estimates. We will use a fixed extinction model for all the Cepheids, but we allow the coefficients to adjust themselves to best fit the data, and the uncertainties in the extinction vector will be included in the distance uncertainties. We constrain the extinction vector  $R_k$  to fit the Cardelli et al. (1989) extinction vector  $R_{0k}$  by adding a Gaussian prior to the likelihood  $\propto \exp(-(R_{0k} - R_k)^2/2\sigma_R^2)$  with  $\sigma_R = 0.1$  and  $R_{0V} = R_V$ . The uncertainty

roughly matches the uncertainties in the Cardelli et al. (1989) model and the differences between various extinction models used for Cepheid distances.

The extinction is not a free variable because it must be positive definite and larger than the estimated foreground extinction (taken from Burstein & Heiles (1984), see Table 1). Freedman et al. (1990, 1992) were the first to face this problem when they found a negative estimated extinction for the Cepheids in M 31 (Baade IV field) and NGC 300, although Sasselov et al. (1996) were the first to use the positivity of the extinction as a constraint when estimating the metallicity dependence of the Cepheid distances from the EROS sample (Beaulieu et al. 1995) of LMC and SMC Cepheids. Most treatments have either advocated raising the mean LMC extinction (Freedman et al. 1992, Böhm-Vitense 1997), ignored the problem (e.g. Saha et al. 1997), or used a statistically incorrect solution in setting  $E = 0$  without changing the distance. When we search for solutions with physical extinctions, we do so by adding a term to the logarithm of the likelihood (eqn. (4)) of the form  $(E_{ki} - E_{fk})^2/\sigma_E^2$  if the extinction  $E_{ki}$  of Cepheid  $i$  in galaxy  $k$  is less than the estimated foreground  $E_{fk}$ , with the scale of  $\sigma_E = 0.045$  set to include the uncertainty in the foreground extinction and the mean LMC extinction. Our choice for the penalty function has the advantage of simplicity, but it rises too abruptly to be an ideal model for global uncertainties in the extinction scale. The structure of the penalty determines the weight attached to Cepheids whose magnitude uncertainties produce negative extinction estimates even if the true extinction is positive. We experimented with several more complicated and mathematically graceful forms for the penalty, but changes in implementation had little effect on the physical results.



### 2.3. Metallicity

There is no debate about the qualitative effects of metallicity on the Cepheids: high metallicity Cepheids are brighter and cooler than low metallicity Cepheids at fixed period. The debate centers only on the magnitude of the effect on distance estimates. The flux is reduced in the blue due to line blanketing, and increased in the red and infrared by backwarming. Theoretical estimates suggest the effect is moderate, about  $(\gamma'_B + \gamma'_V)/2 \simeq 0.14$  mag/dex and  $(\gamma'_B - \gamma'_V) = 0.16$  mag/dex for the mean B and V band luminosity and color (Stothers 1988). Chiosi et al. (1993) find a weaker effect of about  $(\gamma'_V + \gamma'_I)/2 = -0.05$  to  $0.13$  mag/dex in the mean magnitude, and  $(\gamma'_V - \gamma'_I) = 0.05$  to  $0.09$  mag/dex in the  $V - I$  color. An obvious signature of a metallicity dependence in the observational data should be a correlation of Cepheid extinction estimates with the metallicity of the parent galaxy.

Recent attempts to measure the metallicity effects either examined M 31 or compared the LMC and SMC. Freedman & Madore (1990) examined the Cepheids in M 31 where the work of Blair, Kirshner & Chevalier (1982) implied a steep metallicity gradient. They found a distance change with metallicity of  $\delta\mu \simeq (0.32 \pm 0.21)$  mag/dex where the numerical estimate of their gradient is due to Gould (1994). The weak significance of the Freedman & Madore (1990) estimate is used by the Key Project as the basis for neglecting the effects of metallicity in distance estimates pending an analysis of metal rich and metal poor Cepheids in M 101. Gould (1994) also reanalyzed the M 31 data including the empirical covariance matrix of the residuals to find a larger correction of  $(0.88 \pm 0.16)$  mag/dex, although the numerical value depended on the colors used. The low metallicity Baade IV field required a large negative extinction, suggesting that the metallicity requires a color term, as emphasized by Stift (1995) and Sasselov et al. (1996), unless the mean LMC extinction is significantly underestimated (Freedman et al. 1992, Böhm-Vitense 1997). Sasselov et

al. (1996) analyzed the EROS sample of fundamental and overtone Cepheids in the LMC and SMC (Beaulieu et al. 1995) using a method based on Gould (1994) but including both distance and color terms for the metallicity. Unlike the M 31 studies, where the estimate depends on Cepheids of differing metallicity at a common distance, the Sasselov et al. (1996) value relies on positivity of extinction and estimates of the foreground and internal extinctions of the LMC and SMC to estimate the effect. They find a correction of  $0.4_{-0.2}^{+0.1}$  mag/dex in the mean magnitude and  $(0.20 \pm 0.02)$  mag/dex in the V–I color. The color dependence is similar to the Caldwell & Coulson (1986, 1987) and Gieren et al. (1993) estimates for the Galactic Cepheids, of  $(B - V) \propto (0.29 \pm 0.05)$  mag/dex and  $(V - I) \propto (0.20 \pm 0.05)$  mag/dex.

We use the logarithmic abundance of oxygen relative to the LMC (see Table 1,  $\Delta Z = [O/H] - [O/H]_{LMC}$ ) as our metallicity variable because it is the only measured abundance for most of the Cepheid galaxies. Where possible we include the spatial gradients of the metallicity from Zaritsky, Kennicutt & Huchra (1994) and assign metallicities to the Cepheids based on their positions in the galaxy (M 33, M 31, NGC 300, M 81, M 101, NGC 925, NGC 3351, M 100). Where no gradient was available we used a mean metallicity for the whole system (LMC, SMC, IC 4182, NGC 5253, M 96, NGC 4536, NGC 4496A, NGC 4536, NGC 4496A, and NGC 4695). We assigned the Galactic Cepheids a metallicity 0.3 higher than that of the LMC, and we decided not to force a radial metallicity gradient in our current model. For consistency with Freedman & Madore (1990) and Gould (1994) we used the Blair et al. (1982) gradient for M 31 rather than the Zaritsky et al. (1994) gradient. Zaritsky et al. (1994) averaged the Blair et al. (1982) and Dennefeld & Knuth (1981) data even though Blair et al. (1982) strongly disagreed with Dennefeld & Knuth’s (1981) results. We also find an anomalously high metallicity estimate for the M 33 Cepheids compared to M 31. Both of these potential problems could lead to an underestimate of the strength of any metallicity effect.

### 3. Statistical Models of Cepheid Magnitudes and Distances

In this section we build the full model for the Cepheid mean magnitudes, starting from the standard extragalactic method in Model 0. Since the residuals are roughly parallel to the extinction vector, Model 1 allows all Cepheids to have individually estimated extinctions. In Model 2 we allow the Cepheids to have a distribution in temperature at fixed period, and enforce the positivity of the extinction on the models. Finally, we estimate the effects of metallicity in Model 3. We used a flat rotation curve model for the Galaxy to obtain estimates for the solar radius  $R_0$  and circular velocity  $\Theta_0$ . The LMC and SMC are tilted relative to the line-of-sight, have zero width, and their relative distance is determined between the (bar) centers. The tilt is optimized as part of the solution and agrees well with Caldwell & Laney (1991). To facilitate comparisons with the standard PL relations of Madore & Freedman (1991), we assume an LMC distance modulus of 18.5 mag and a mean LMC extinction of  $E(B - V) = 0.10$ , but we have shifted the period origin to  $\log P_0 = 1.4$ . We only discuss the results for the Johnson UBV, Kron-Cousins RI, and Glass-Carter JHK bands.

#### 3.1. Model 0: The Standard Method

We start our analysis by considering the Cepheid correlation functions in the absence of metallicity ( $\gamma'_k = 0$ ), scatter in the temperature ( $\beta_k = 0$ ), and allow only the Galactic Cepheids to have individually determined extinctions. Model 0 treats all the extragalactic Cepheids using the standard extragalactic method. The parameters for the PLC relations and their uncertainties are summarized in Table 2, and the derived distances and mean extinctions for the extragalactic samples are summarized in Table 3. Our zero-points and period slopes are in general agreement with Freedman & Madore (1991). The zero-points are approximately 0.04 mag and 0.02 mag fainter in the critical V and I bands, but

the differences lie well within the standard uncertainties. Our PL relation slopes  $\alpha'_k$  are uniformly shallower by 0.05–0.10, although the agreement is again consistent with the uncertainties in the individual estimates. The zero-points and slopes agree with recent studies by Laney & Stobie (1994)<sup>1</sup> and Tanvir (1996).<sup>2</sup> The best fit extinction vector differs from the nominal Cardelli et al. (1989) vector by  $0.15 \pm 0.08$ ,  $-0.01 \pm 0.06$ ,  $-0.07 \pm 0.05$ ,  $-0.05 \pm 0.05$ ,  $+0.10 \pm 0.06$ ,  $+0.02 \pm 0.06$ , and  $0.08 \pm 0.06$  for U, B, R, I, J, H, and K respectively. The changes in the coefficients are not a simple change in the  $R_V$  value of the Cardelli et al. (1989) model, and the final uncertainties in the  $R_k$  are less than the uncertainties in the prior. The ratio  $A_V/A_I = 1.63 \pm 0.05$  lies between the Key project ( $A_V/A_I = 1.6$ ) and SN Ia ( $A_V/A_I = 1.7$ ) values. The shifts in the Glass-Carter JHK coefficients were expected, because we lacked the true mean effective wavelengths for these filters and had simply set their values to those for the CTIO JHK filters. However, the sign of the shift is opposite to that found by Laney & Stobie (1993), who found smaller extinction coefficients using a different analysis technique.

Our distance estimates generally agree with the published values (see Tables 3 and 4, and Figures 1 and 2a) with a few exceptions. We find that M 31, M 33, and NGC 300 are closer than the published values by  $-0.11$ ,  $-0.12$ , and  $-0.05$  magnitudes respectively. In M 33 the reason is the significantly higher extinction estimate of  $E(B - V) = 0.16$  instead of 0.10. Both earlier Cepheid distance estimates for M 33 (Freedman 1985, Madore et al. 1985), and other models tested in Freedman et al. (1991) match our higher extinction

---

<sup>1</sup> Laney & Stobie (1994) found zero-points of  $V_{0k} = 13.28 \pm 0.09$ ,  $11.90 \pm 0.06$ ,  $11.47 \pm 0.06$ , and  $11.38 \pm 0.06$  mag and PL slopes of  $\alpha'_k = -2.87 \pm 0.07$ ,  $-3.31 \pm 0.05$ ,  $-3.42 \pm 0.05$ , and  $-3.44 \pm 0.05$  in the V, J, H, and K bands for a mean LMC modulus of 18.5 mag

<sup>2</sup> Tanvir (1996) found zero-points of  $V_{0k} = 13.24 \pm 0.04$  and  $12.45 \pm 0.03$  and PL slopes of  $\alpha'_k = -2.774 \pm 0.083$  and  $-3.039 \pm 0.059$  for V and I.

estimates. Since the Cepheid distances to M 31 and M 33 calibrate many other distance indicators, these shifts would increase some estimates of the Hubble constant by 6–7%. Our agreement with the Key Project estimates is excellent, with a mean shift of  $-0.05$  mag, similar to that found by Tanvir (1996) due to zero-point recalibration. Our error and extinction estimates are also in good agreement, except for M 81 where we find a significantly higher mean extinction of 0.075 (the Key Project value of 0.03 is less than the estimated foreground extinction of 0.04). For M 96, we agree with the values for the distance and mean extinction found by Tanvir et al. (1995), but we derive much larger uncertainties of 0.28 (versus 0.16) mag for the distance and 0.12 (versus 0.03) for the extinction. We found significant disagreements with the Type Ia project in the distance estimates, extinction estimates and uncertainties. On average our distances were  $-0.09$  mag smaller, the extinctions were 0.04 larger, and our distance uncertainties were generally twice as large. The results significantly change the zero-point of the MLCS SNIa distance scale (Riess et al. 1996), since the distances to the calibrators 1972E in NGC 5253, 1981B in NGC 4536, and 1990N in NGC 4639 are revised from  $28.08 \pm 0.10$  mag to  $27.70 \pm 0.32$ ,  $31.10 \pm 0.13$  to  $30.97 \pm 0.22$ , and  $32.03 \pm 0.22$  to  $32.11 \pm 0.32$  respectively. The revised MLCS estimate of the Hubble constant is  $69 \pm 8$  km s $^{-1}$  Mpc $^{-1}$ , an 8% increase from the original estimate of  $64 \pm 6$  km s $^{-1}$  Mpc $^{-1}$ . Some of the differences may be due to our use of a consistent extinction law for all the galaxies (the Type Ia project uses the Madore & Freedman (1991) PL relation based on  $R_V/R_I = 1.6$  but fit the data using  $R_V/R_I = 1.7$ ), and our use of statistically consistent treatments of the covariance between distance and extinction. For example, in NGC 5253 Saha et al. (1995) give large uncertainties in the extinction (see Table 3) that are statistically inconsistent with the small uncertainties in the distance. Figure 2 compares two absolute distance estimates, the expanding photosphere method for Type II supernovae (Eastman et al. 1996) and physical models of Type Ia supernovae (Höflich & Khokhlov 1996), and two relative distance estimates, surface

brightness fluctuations (Tonry 1996) and the MLCS/SNIa (Riess et al. 1996) method, to the Cepheid distances (see Table 4).

Magnitude selection biases may be important in Model 0 because of the large scatter in the PL relations. Biases have been extensively discussed in the literature, most recently by Tanvir (1996), along with debates on how to optimally perform model fits (e.g. fitting inverse PL relations as in Kelson et al. (1996)). We can avoid the biases almost completely by using PLC relations to model the correlations in the residuals and to reduce the intrinsic scatter. Since these approaches are also physically more useful, we will not discuss selection biases further.

### 3.2. Model 1: Scatter In the Extinction

The magnitude residuals of all the extragalactic Cepheids are highly correlated and lie along the extinction direction (see Figure 3).<sup>3</sup> The importance of allowing individual extinctions is glaringly obvious if we compare the residuals for the Galactic and extragalactic samples – for the Galactic Cepheids there are 624 measured mean magnitudes for 121 Cepheids with an rms residual of 0.06 magnitudes, while for the extragalactic Cepheids

---

<sup>3</sup>Contrary to the conclusions of the Type Ia project, we find that the residuals in IC 4182, NGC 4536, NGC 4496a and NGC 5253 are also correlated with the extinction vector. We believe their conclusion is an artifact of examining residuals in the space of  $\Delta V - \Delta I$  versus  $\Delta V$ . Both the mathematics of the covariance matrix and simple experiments show that when the uncertainties in  $I$  are larger than those in  $V$ , the  $\Delta V - \Delta I$  versus  $\Delta V$  covariance diagrams can look symmetric and uncorrelated even when the data is correlated. The quantity  $\Delta V - \Delta I$  simultaneously reduces the signal from differential extinction and increases the apparent noise (see Fig. 3).

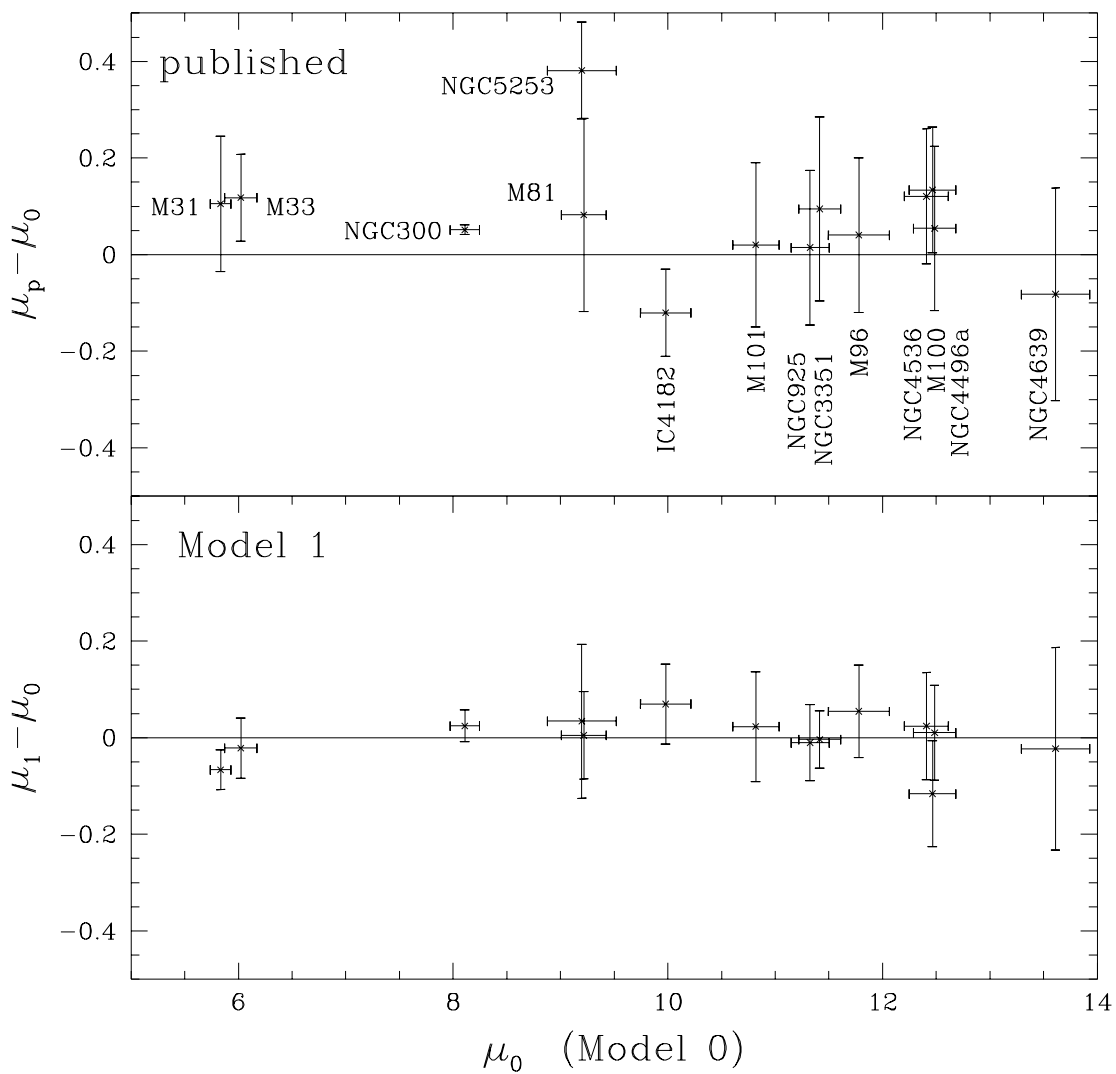


Fig. 1.— Distance comparisons between Model 0 and either published (top) or Model 1 (bottom) distances. The horizontal error bar is the error in Model 0, while the vertical error bar is the error in the comparison distance.

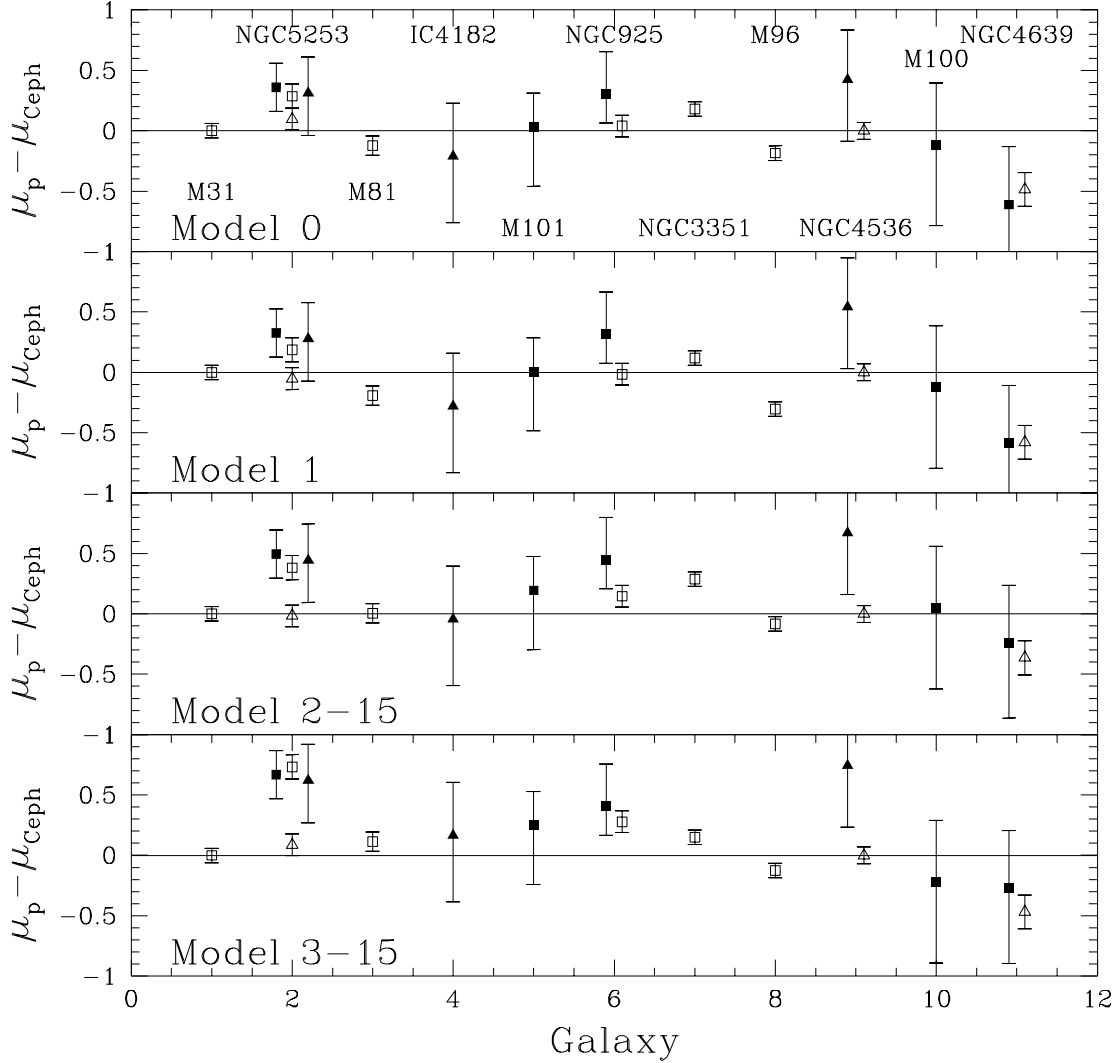


Fig. 2.— Distance comparisons to other methods. The expanding photosphere method for SNIa (EPM, solid squares, Eastman et al. 1996) and physical models of SNIa (SnIa, solid triangles, Höflich & Khokhlov 1996) are absolute distances. The surface brightness fluctuation distances are shown relative to M 31 (SBF, open squares, Tonry et al. 1996) and the SNIa/MLCS method distances are shown relative to NGC 4536 (MLCS, open triangles, Riess et al. 1996). The error bars are the uncertainties in the non-Cepheid distance indicator.



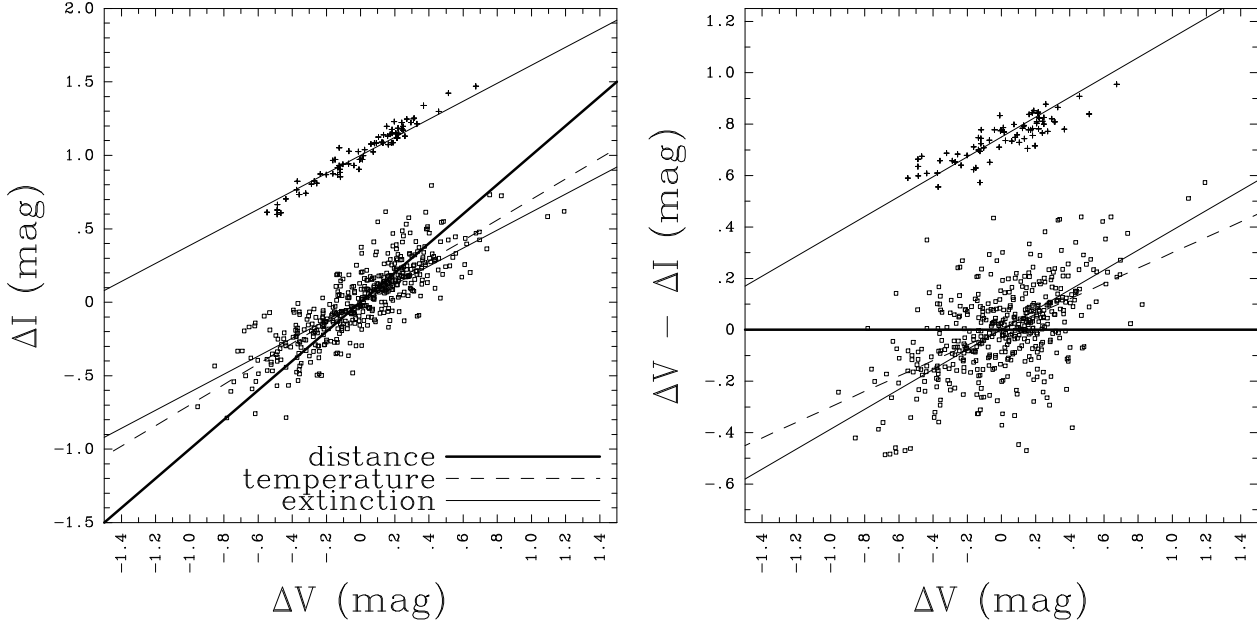


Fig. 3.— Magnitude residuals in Model 0. The left panel is a simple diagram of the  $\Delta V$  and  $\Delta I$  residuals (squares). It shows that the residuals are strongly correlated and lie roughly along the extinction vector. The right panel displays the same residuals using the  $\Delta V$  versus  $\Delta V - \Delta I$  format of Type Ia project. The correlation, while still clearly present, is much more difficult to recognize. We also display the residuals (vertically offset, crosses) and the extinction direction for the more accurately measured LMC and SMC Cepheids to illustrate the effects of measurement uncertainties on the apparent correlations. The heavy solid, dashed and light solid lines show the expected directions for distance, temperature and extinction residuals respectively.

there are 1617 magnitudes for 545 Cepheids with an rms residual of 0.29 magnitudes. The independent distance and extinction estimates for the Galactic Cepheids dramatically reduce their residuals compared to the rest of the sample even though a large subset of the Galactic Cepheids have 5 to 8 color photometry while most of the extragalactic Cepheids have only two color photometry.

In Model 1 we allow all Cepheids an independent extinction variable, as we have already used for the Galactic Cepheids in Model 0. Each Cepheid  $i$  in galaxy  $k$  was assigned extinction  $\langle E_k \rangle + \Delta E_{ki}$ , where  $\langle E_k \rangle$  is the mean extinction and the correction  $\Delta E_{ki}$  is forced to have zero mean for each galaxy and is limited by a Gaussian prior whose width  $\sigma_{Ek}$  is simultaneously optimized. We need the prior because most of the extragalactic Cepheids have only two filters, and as we start assigning each Cepheid individual extinctions, temperatures and metallicities we will overfit the data if we do not include the covariance matrix (eqns. 4 and 5) and optimize the priors. Some extragalactic distance estimates have used of individual extinction estimates (e.g. Tanvir et al. 1995) or reddening free magnitude estimates (e.g. Freedman et al. 1990, 1991, 1992, Saha et al. 1996ab, 1997), although the final distance estimates are usually based on the standard PL relations. These individual extinction estimates correspond to taking the limit  $\sigma_E \rightarrow \infty$  in eqns. (4) and (5), and they may overestimate the width of the extinction distribution in noisy data.

The changes in the Cepheid relations and distances are summarized in Tables 2 and 3 and Figure 1. In Model 1 the rms residuals for the extragalactic Cepheids drop to 0.09 mag from 0.29 mag in Model 0. The rms residuals for the LMC and SMC (0.06 and 0.08 mag) are smaller than the other extragalactic systems (0.10 mag) even though the average Cloud Cepheid was measured in 5 filters. The removal of the extinction-correlated residuals leads to large reductions in the PLC relation widths (which represent uncorrelated errors), but the residuals are still correlated (particularly UJHK) and the PLC widths are still broader

than expected given the estimated measurement errors. The zero-points and slopes show little change from Model 0 and have reduced uncertainties, but the estimated extinction vector has changed considerably in the infrared, suggesting that it has absorbed some of the variance due to temperature as well as extinction. In particular, the distance of the sun from the Galactic center ( $R_0$ ) is strongly affected by the change in the IR extinction coefficients (from 7.5 kpc to 6.7 kpc).

As Figure 3 illustrates, the extinction and temperature are very nearly parallel for V and I, so it is very difficult to cleanly separate the two physical terms in noisy two-color data. Madore & Freedman (1991) question whether the two variables can be accurately separated even with more accurate three-color data used for Galactic Cepheid extinction estimates, although their position is strongly rejected by Laney & Stobie (1993, 1994). Moreover, the HST Cepheid data may have correlated systematic errors due to crowding, differences in analysis methods, and the construction of the I mean magnitude using the V light curves for interpolation that Model 1 interprets as extinction variations. Such systematic errors have no effect on the distance estimates, since correlated residuals must be modeled for a correct statistical treatment, but they may strongly affect our interpretation of the scatter in terms of extinction. Note, however, that the spread in color in the extragalactic systems is quite comparable to the spread in the Magellanic Clouds (Figure 3), and it would be truly astonishing if the extinction from a large sample of objects randomly chosen from spiral galaxies failed to show significant scatter.

Other than the value of  $R_0$ , the distances are little changed from Model 0 (see Fig. 1), with a mean shift of less than 0.01 mag. The typical distance and mean extinction uncertainties, however, are roughly half those of Model 0, although the reduction is most dramatic for galaxies with small numbers of Cepheids (e.g. M 96). The change is largely due to the reduced rms magnitude residual in estimating the intrinsic Cepheid luminosities.

In Model 0 the statistical uncertainty is  $\sim 0.29/N^{1/2}$  magnitudes where the numerical coefficient is the combination of the measurement errors and the PLC relation width, while in Model 1 the typical uncertainty is  $\sim 0.10/N^{1/2}$  magnitudes. The total uncertainties are larger due to calibration uncertainties in the PLC relations and the HST magnitudes that are unaffected by statistical averaging. Fitting the correlated residuals also makes our model significantly less sensitive to magnitude selection biases than Model 0, although the general agreement of the results suggest they were not of great importance. The MLCS estimate of the Hubble constant becomes  $72 \pm 6 \text{ km s}^{-1} \text{ Mpc}^{-1}$ , slightly higher than in Model 0. Figure 2 compares the Cepheid distances to the distances in Table 4.

### 3.3. Model 2: Temperature and the Positivity of the Extinction

Figure 4 shows the mean extinctions relative to the foreground extinction and the width of the extinction distribution as a function of the metallicity of the host galaxy. The Model 1 solutions are unphysical because many of the galaxies have either negative mean internal extinctions (SMC, NGC 300, IC 4182 and NGC 4639) or extinction distributions extending to negative internal extinctions. Even for the LMC and the SMC, where we have many filters, good accuracy, and no systematic problems such as the HST calibration terms, there are Cepheids with extinctions less than the expected foreground extinction. The simplest solution to the problem, and the one advocated by Freedman et al. (1992) when they first faced the problem for the NGC 300 Cepheids and more recently advocated by Böhm-Vitense (1997), is simply to raise the mean LMC extinction from the standard  $\langle E \rangle_{LMC} = 0.10$  assumed in the extragalactic Cepheid analyses. Both Freedman et al. (1992) and Böhm-Vitense (1997) suggest that the problem can be solved by increasing the mean extinction to  $\langle E \rangle_{LMC} \simeq 0.18$ . Our larger sample and the interpretation of the scatter in color as an extinction distribution increases the required LMC extinction to

$\langle E \rangle_{LMC} \gtrsim 0.25$ . The standard Galactic Cepheid analyses derive mean LMC extinctions of only 0.07 (e.g. Caldwell & Coulson 1986), even lower than  $\langle E \rangle_{LMC} = 0.10$ , based on a combination of the Cepheid colors and other estimates of the space reddening. Grieve & Madore (1986) found median LMC supergiant extinctions of approximately 0.10, with 90% of the estimated extinctions below  $E(B - V) = 0.18$ . Bessel (1991), in arguing for higher than generally accepted extinctions for the LMC and SMC, advocates an increase to only  $\langle E \rangle \sim 0.13$  based on HI column densities, optical polarization, interstellar absorption lines, and color excesses. Thus the trivial solution to the negative extinction problem of simply raising  $\langle E \rangle_{LMC}$  can only be a partial solution. As Freedman et al. (1992) also noted, the temperature distribution at fixed period contributes to the negative extinction problem if the two variables are not distinguishable and hotter than average Cepheids are assigned reduced extinctions.

In Model 2 we try to minimize the effects of the temperature distribution in biasing the extinctions by giving each Cepheid a temperature deviating by  $\delta t$  from the mean for its period, constrained by a Gaussian prior of width  $\sigma_{PC}$  corresponding to the width of the instability strip (see eqn. 2). We also force the extinctions to be positive by adding the extra terms to the likelihood function discussed in §2.2. Since there is some uncertainty in the extinction normalization, we explore three models with  $\langle E \rangle_{LMC} = 0.10, 0.15,$  and  $0.20$  labeled by Model 2–10, 2–15, and 2–20, that correspond to low, slightly high, and very high estimates for the mean extinction. We adopt Model 2–15 as our standard, and the resulting PLC vectors, distances, and extinctions are presented in Tables 2 and 3. In Model 2 we must determine the temperature vector  $\beta_k$  as well as the temperature corrections,  $\delta t$ , and as is frequently noted in the extragalactic critiques of the Galactic Cepheid methods (e.g. Madore & Freedman 1991), the temperature state vector  $\beta_k$  is hard to determine uniquely from the mean magnitudes. Indeed, we found that we could not stably estimate  $\beta_k$  without including a prior based on the variation of color with phase. Based on an

analysis of Cepheid light curves (Kochanek 1997b), we estimated a model  $\beta_{0k}$  (see Table 2), assumed that the uncertainty in the coefficients was 0.05, and added a Gaussian prior for the deviation of  $\beta_k$  from  $\beta_{0k}$  to the likelihood. We should note, however, that many of the Galactic analyses use a very similar approach to calibrating the PLC relations (e.g. Laney & Stobie 1986, 1993, 1994). The need to make such a strong assumption about  $\beta_k$  combined with (or due to) the limited two-color photometry on most of the extragalactic systems is a primary limitation for the remainder of our analysis, but the simultaneous optimization of the prior widths keeps us from overfitting the data.

We find a width for the instability strip of  $\sigma_{PC} \simeq 0.18 \pm 0.01$  in all three models, which corresponds to a FWHM in the V–I (B–I) colors at fixed period of 0.08 (0.14) mag. Unlike the previous two models, Model 2 gives non-zero values for HST calibration variables ( $\Delta V, \Delta I$ ) of  $(0.05 \pm 0.04, -0.04 \pm 0.04)$ ,  $(0.03 \pm 0.04, -0.03 \pm 0.04)$ ,  $(0.02 \pm 0.04, -0.03 \pm 0.04)$  for Models 2–10, 2–15, and 2–20 respectively. In all three cases the calibration uncertainties provide a significant part of the solution to the negative extinction problem. Note that the PLC zero points for Model 2-15 are not directly comparable to the previous models due to the change in the extinction. The infrared extinction coefficients are now closer to the priors than in Model 1 and agree with the Laney & Stobie (1993) estimates and the estimated value of  $R_0 = 7.7 \pm 0.3$  kpc is again consistent with other estimates (Reid 1993).

Standard Cepheid distances are *biased* distance estimators because they treat positive and negative extinctions equally. The sense of the bias is always to overestimate the distances, because lower extinctions correspond to higher distances. Random photometry errors can and will produce negative extinctions for objects with positive extinctions, but such problems affect only the mathematics of implementing the positive extinction condition, not the need for it. Any procedure to impose the physical condition that the extinction is positive must reduce the likelihood for large distances and thereby drive the

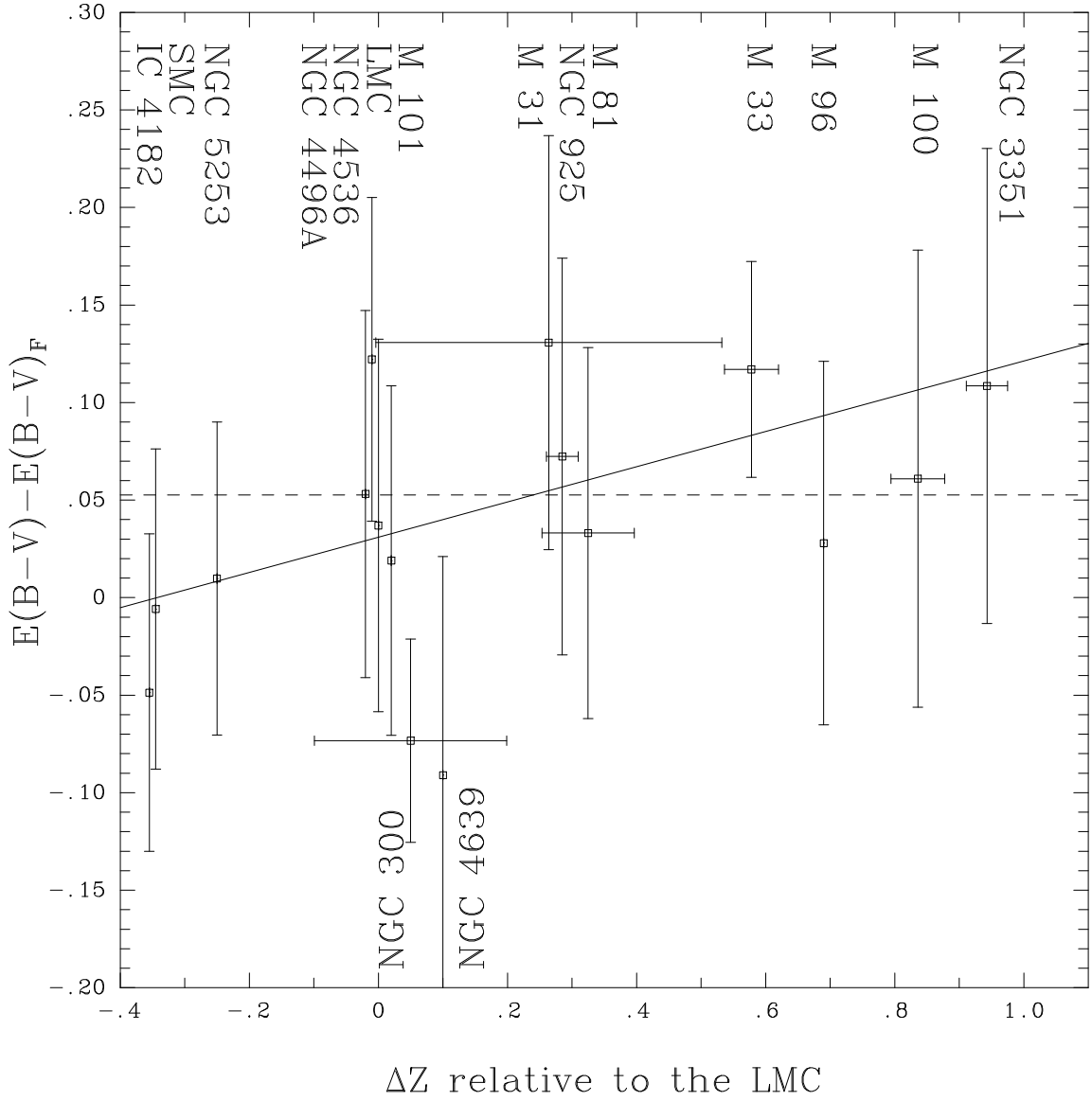


Fig. 4.— Extinctions and metallicity. The points for each galaxy show the mean extinction relative to the foreground extinction  $\langle E_k \rangle - E_{fk}$  and the width of the extinction distribution  $\sigma_{E_k}$  for Model 1 as a function of the metallicity. The uncertainty in the mean extinction is smaller than  $\sigma_{E_k}$  by roughly the square root of the number of Cepheids in the galaxy (see Table 3). The metallicity error bars show the spread in the metallicities of the Cepheids used in the model. The solid and dashed lines show the best linear and constant fits for the trend excluding NGC 300 and NGC 4639. Several points have been shifted slightly in metallicity to separate the vertical error bars.

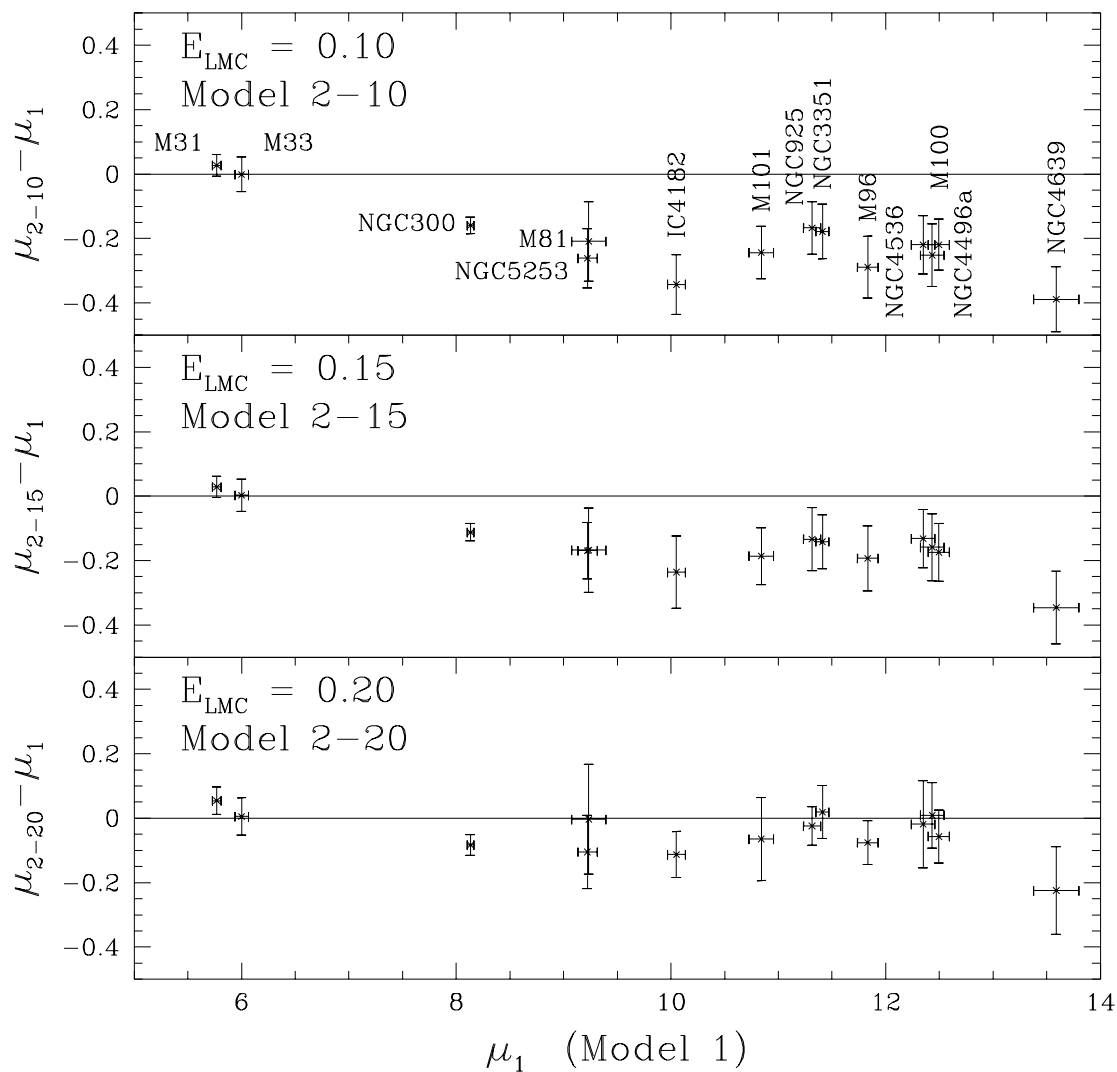


Fig. 5.— Distance comparisons between Model 2 and Model 1 distances for the low (top), middle (center) and high (bottom) LMC extinction estimates. The horizontal error bar is the error in Model 1, while the vertical error bar is the error in Model 2.



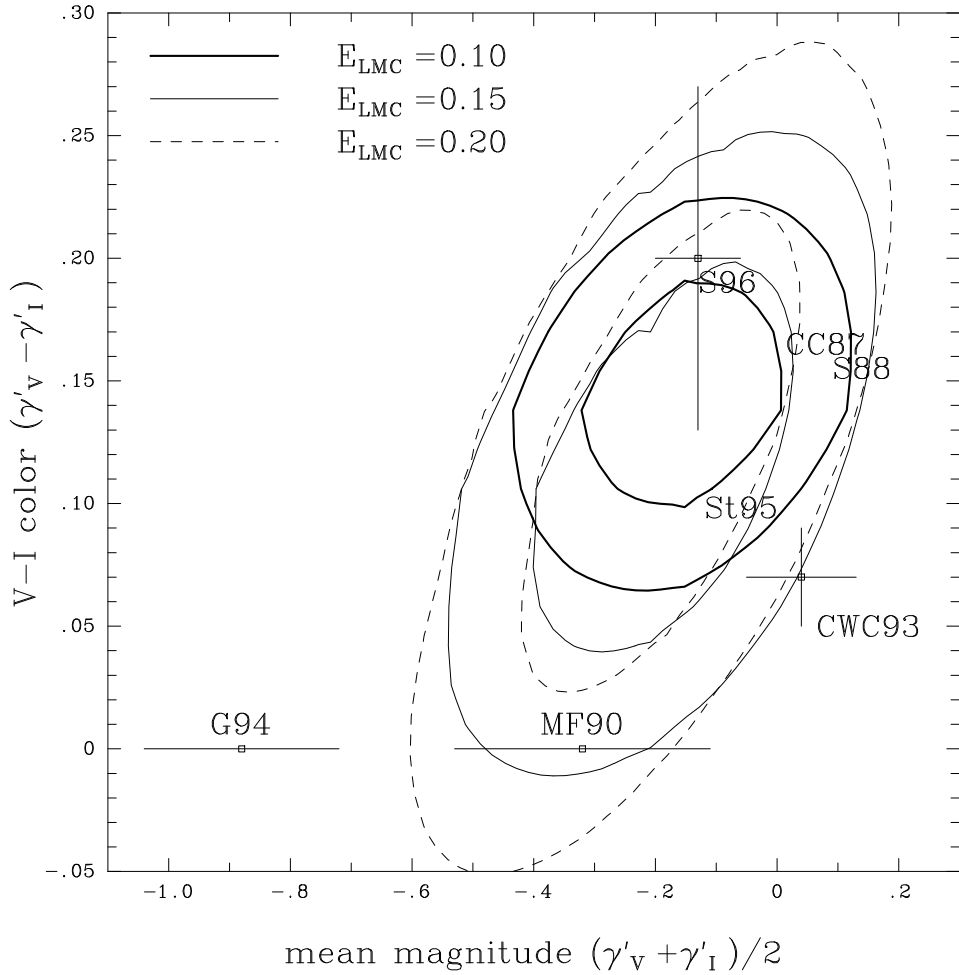


Fig. 6.— Metallicity corrections to the zero point. Likelihood contours for the change in mean magnitude  $((\gamma'_V + \gamma'_I)/2)$  and V-I color  $(\gamma'_V - \gamma'_I)$  compared to other observational and theoretical determinations. The contours are the 1- $\sigma$  ( $\Delta\chi^2 = 2.30$ ) and 2- $\sigma$  ( $\Delta\chi^2 = 6.17$ ) confidence intervals for two parameters. The G94 (Gould 1994) and MF90 (Madore & Freedman 1990, as estimated by Gould 1994), estimates included no color variation. CWC93 marks the theoretical estimate for V-I from Chiosi et al. (1993). S88 and St95 mark the theoretical estimates for B-V from Stothers (1988) and Stift (1990, 1995). CC87 marks the semi-empirical model for B-V from Caldwell & Coulson (1987). S96 marks the Sasselov et al. (1996) V and I determination from the EROS Cepheids.

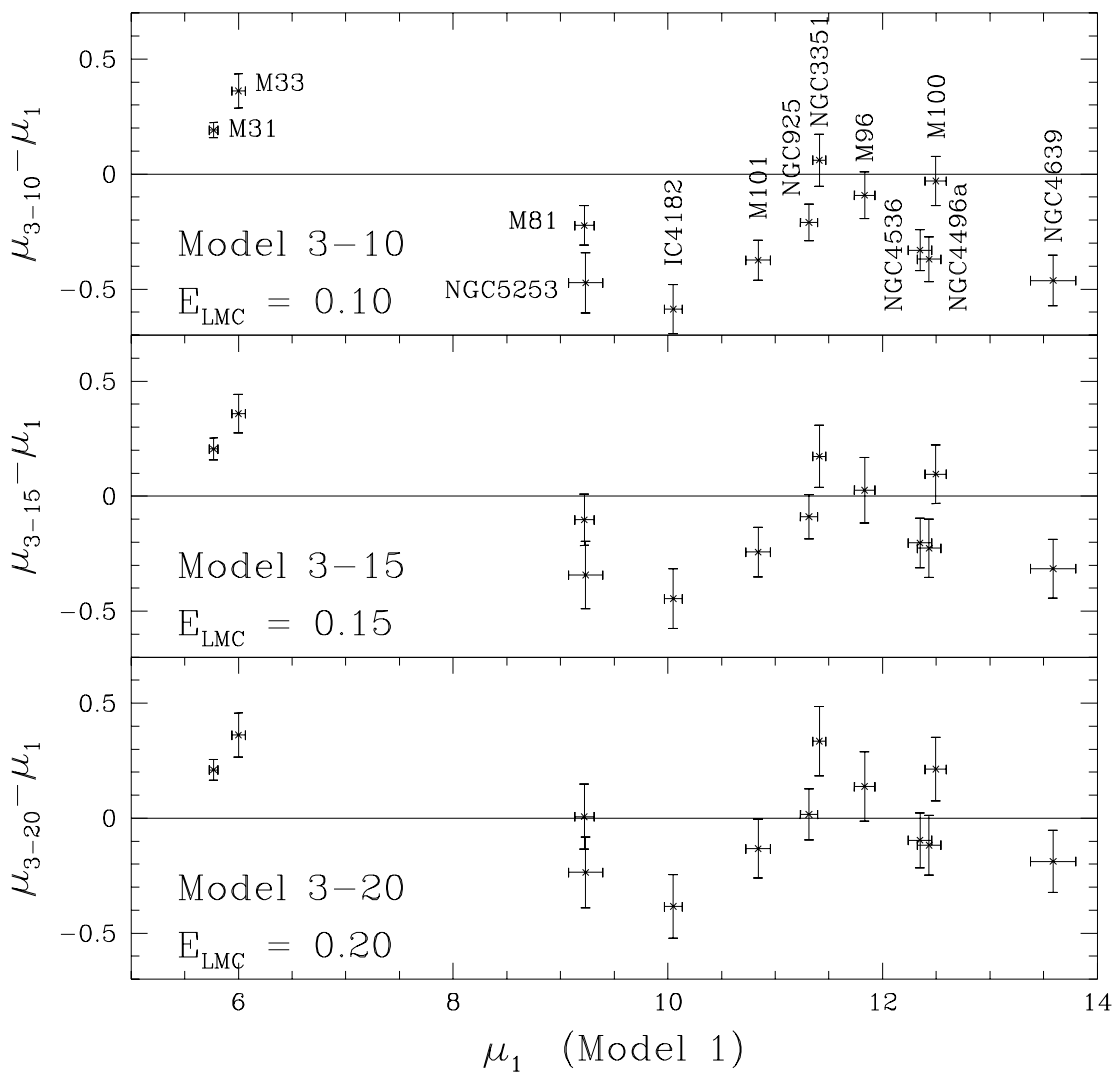


Fig. 7.— Distance comparisons between Model 3 and Model 1 distances for the low (top), middle (center) and high (bottom) LMC extinction estimates. The horizontal error bar is the error in Model 1, while the vertical error bar is the error in Model 3.

best fit distance estimate downwards. It is also a global bias, because the Cepheid distance and extinction estimates are tightly correlated by the PLC relations. When we force a galaxy with strongly negative extinction estimates like NGC 300 to have a higher extinction and a lower distance, the correlations caused by all the Cepheids sharing the same estimate of their intrinsic colors will also force galaxies like M 33 with strictly positive extinctions to higher extinctions and lower distances as well. *Adjusting the extinction of one galaxy without adjusting the extinction of all galaxies is physically and statistically incorrect, unless the reason for the adjustment is a systematic error in the data for that particular galaxy.* The negative extinction problems should not be solved “locally.”

As Figure 5 shows, Model 2 simply drives the galaxies to lower distances and higher extinctions, until it is reasonably unlikely that any Cepheids have negative extinctions. The mean distances shift by  $-0.20$ ,  $-0.14$ , and  $-0.05$  mag for Models 2–10, 2–15, and 2–20 respectively, with the low LMC extinction Model 2–10 requiring the largest shift. The effect is strongest on the low metallicity galaxies, which means the changes in the MLCS calibrations are considerable. The MLCS Hubble constant estimates are  $80 \pm 6$ ,  $78 \pm 6$ , and  $72 \pm 6$  km s $^{-1}$  Mpc $^{-1}$  for the three models compared to  $72 \pm 6$  km s $^{-1}$  Mpc $^{-1}$  for Model 1. Because the effects of the bias are global, even a relatively high extinction galaxy like M 100 is driven to lower distances. Scaling from the Mould et al. (1995) estimate of 80 km s $^{-1}$  Mpc $^{-1}$ , which becomes 82 km s $^{-1}$  Mpc $^{-1}$  in Model 1, the Hubble constant shifts to  $H_0 = 90$ , 88, and 84 km s $^{-1}$  Mpc $^{-1}$  in Models 2–10, 2–15, and 2–20 respectively.<sup>4</sup> Despite the large shifts, the agreement with other distance indicators (see Fig. 2) is no worse than in Model 1, if only because the absolute distance indicators have low accuracy while the relative distances are almost unchanged. The goodnesses of fit for Model 2 are considerably

---

<sup>4</sup>The uncertainties in the  $H_0$  estimate from M 100 are dominated by the systematic uncertainties in the model for Virgo (Mould et al. 1995).

worse than Model 1, even though we have allowed separate temperature estimates for the Cepheids. The likelihood function has increased by  $\Delta 2 \ln L = 139, 78,$  and  $65$  relative to Model 1, despite *adding* 695 new degrees of freedom to the model!

### 3.4. Model 3: Metallicity

The Model 2 solutions are not very attractive because of the huge downward shifts in the distances, and the association of unphysical extinctions with low metallicity in Figure 4 strongly suggests the need for a metallicity dependence in the Cepheid distance. In Model 3 we add a metallicity dependence to the Cepheid zero-point vector  $\gamma'_k$ , as in the model of Sasselov et al. (1996). The formal trend of extinction with metallicity (neglecting NGC 300 and NGC 4639) corresponds to a color dependence of  $V - I \propto (0.09 \pm 0.01)\Delta[O/H]$ , which is comparable to the color variations predicted in theoretical models (e.g. Stothers 1988, Stiff 1990, Chiosi et al. 1983) and previous experimental estimates (e.g. Gieren et al. (1993), Sasselov et al. (1996)). There are, however, two discrepant points in Figure 4, NGC 300 and NGC 4639, both of which are significantly bluer than the trend. For NGC 4639 the large uncertainties in the extinction can probably explain the discrepancies. NGC 300 is peculiar, and we drop it from our subsequent analysis – in doing so, we are assuming that the blue color of the Cepheids is either an artifact of the Freedman et al. (1992) data or that the HII region abundance estimates are incorrect.

In Model 3 we added the metallicity dependent zero-point correction  $\gamma'_k \Delta Z$  to Model 2, and repeated the calculation for the three different mean LMC extinctions labeled by Model 3–10, 3–15, and 3–20. As in Model 2, we present the full results only for Model 3–15 in Tables 2 and 3. We fit the data leaving the input metallicities fixed ( $\sigma_Z \rightarrow 0$ ), because attempting to determine the metallicities from the data was unjustified by the amount and quality of the data. If we have found a solution for the distance modulus  $\mu_1$  and extinction

$E_1$  ignoring the metallicity zero point correction  $\gamma'_k$ , then the true distance modulus is

$$\mu_0 = \mu_1 - \frac{\gamma'_V + \gamma'_I}{2} \Delta Z + \frac{\gamma'_V - \gamma'_I}{2} \frac{R_V + R_I}{R_V - R_I} \Delta Z \quad (9)$$

and the true extinction is

$$E_0 = E_1 - \frac{\gamma'_V - \gamma'_I}{R_V - R_I} \Delta Z \quad (10)$$

where the terms are broken into the change in the mean V and I magnitudes and the change in the V–I color. If low metallicity Cepheids are blue ( $\gamma_V - \gamma_I > 0$ ) then adding the metallicity term can solve the extinction problem without driving the distances of all galaxies downwards as in Model 2. The metallicity terms will not, however, change the embarrassingly low distances to the low metallicity galaxies in Model 2, because their distances are still reduced by  $(R_V + R_I)/2 \sim 2.7$  times the change in the extinction.

Our solutions generically made the metal rich Cepheids redder and brighter than the metal poor Cepheids, as shown in Figure 6. The best fit solution changes little with the assumptions about the LMC extinction, and the absence of a metallicity dependence is ruled out at greater than 95% confidence. The mean luminosity changes in the V and I bands,  $(\gamma'_V + \gamma'_I)$ , are  $-0.13 \pm 0.09$ ,  $-0.15 \pm 0.14$ , and  $-0.17 \pm 0.15$  mag/dex for Models 3–10, 3–15, and 3–20 respectively, and the mean changes in color,  $\gamma'_V - \gamma'_I$ , are  $0.15 \pm 0.03$ ,  $0.13 \pm 0.04$ , and  $0.15 \pm 0.07$  respectively. The less strongly we restricted the permitted range for the extinctions, the more uncertain the metallicity dependence. As pointed out by Sasselov et al. (1996), the positivity of the extinction is an important component in the quantitative determination of composition effects. The HST calibration uncertainties still represent a major problem, and they contribute much of the solution to maintaining positive extinctions. The calibration variables  $(\Delta V, \Delta I)$  are  $(0.09 \pm 0.04, -0.07 \pm 0.04)$ ,  $(0.05 \pm 0.04, -0.05 \pm 0.04)$ , and  $(0.03 \pm 0.04, -0.03 \pm 0.04)$  for the three solutions. The overall structure of the metallicity vector  $\gamma'_k$  matches theoretical expectations. Metal rich Cepheids show a decreased flux in U and B, and then a gradually increasing flux in the

redder bands, reaching a plateau in the infrared. The uncertainties in the  $\gamma'_k$  in Table 2 are dominated by the uncertainties of the mean luminosity change, and as the error ellipses in Figure 6 demonstrate, the uncertainties in the color changes are considerably smaller.

Most of the debate about composition effects on extragalactic Cepheid distances has focused on the M31 Cepheids studied by Madore & Freedman (1990) and Gould (1994). These models allowed no color changes due to composition ( $\gamma'_k = \gamma'_j$ ), while it is clear both from theoretical models, previous experimental estimates, and our estimates, that the changes in color are the dominant source of changes in distance estimates. Our estimates of the effect are slightly higher than the theoretical estimates of Chiosi et al. (1993). The B–V color change of 0.28 mag/dex is not as well constrained because most of the galaxies lack B photometry, but it is larger than the theoretical estimates of Stothers (1988) and Stift (1990, 1995). The values match the experimental determination by Sasselov et al. (1996) using the EROS sample of Cepheids in the LMC and SMC and the typical Galactic Cepheid metallicity correction models (e.g. Caldwell & Coulson 1986, 1987, Gieren et al. 1993).

Figure 7 shows the changes in the distances relative to Model 1 for the three different assumptions about the LMC extinction. As expected, the metal poor galaxies (e.g. NGC 5253, IC 4182, NGC 4536) are shifted to lower distances relative to the metal rich galaxies (e.g. NGC 3351, M 33, M 100). The mean change in distance depends on the mean extinction of the LMC, with Model 3–10 still requiring a significant reduction in the mean distances. The MLCS estimates of the Hubble constant become  $85 \pm 6$ ,  $80 \pm 6$  and  $79 \pm 6$  km s<sup>-1</sup> Mpc<sup>-1</sup> for Models 3–10, 3–15, and 3–20 respectively, while the estimates based on M 100 (Mould et al. 1995) are 83, 78 and 74 km s<sup>-1</sup> Mpc<sup>-1</sup> respectively. The metal poor calibration (MLCS) moves to lower distance and higher Hubble constant, while the metal rich calibration (M 100) moves to higher distances and lower Hubble constants. The comparison with other distance indicators (Figure 2) is no worse than the other cases,

with the exception of NGC 5253.

#### 4. Conclusions

We have systematically explored the problem of extragalactic Cepheid distances and their primary systematic errors. While the details of some of the model implementations are certainly open to criticism, we have tried to include or illustrate all the principal uncertainties. When we implement the standard extragalactic analysis method (Madore & Freedman 1991) in Model 0, we find general agreement with existing distances, with significant corrections only for the Type Ia supernova calibration galaxies. Our revised, distances to the SNIa MLCS (Riess et al. 1996) calibrating galaxies NGC 5253, NGC 4536, and NGC 4639 produce a revised Hubble constant estimate of  $69 \pm 8 \text{ km s}^{-1} \text{ Mpc}^{-1}$ . Our new distance estimates and uncertainties have the advantages of a homogeneous statistical treatment, a standard extinction model, and the inclusion of the full uncertainties in the extinction and Cepheid model on the distances. In Model 0, the magnitude residuals for all galaxies are strongly correlated with the extinction vector, and when we allow each Cepheid an individual extinction in Model 1, the typical magnitude residual drops from 0.29 mag to 0.09 mag. The Galactic Cepheid community (e.g. Caldwell & Coulson 1986, 1987, Caldwell & Laney 1991, Fernie 1990, Fernie et al. 1995, Laney & Stobie 1993, 1994, 1996) includes individual extinctions as a matter of routine. Some extragalactic studies effectively fit individual extinctions or use reddening free magnitudes (e.g. Tanvir et al. 1995, Freedman et al. 1990, 1991, 1992, Saha et al. 1996ab, 1997), but they are usually not used in the final distance estimate. As the sadly neglected work of Gould (1994) emphasized, a correct statistical model must include the effects of these correlations on the uncertainties in the distance *independent of the physical interpretation for their origin*. The danger of confusing extinction, temperature, and correlated systematic errors affects only the interpretation

of the model not the need to account for correlated residuals. Including the correlations does not change the values for the distances and mean extinctions, but it does significantly reduce their uncertainties (see Figure 1).

In both of these models, many Cepheids require negative intrinsic extinctions for the host galaxies, which is clearly unphysical. The simple solution to the problem is to raise the mean LMC extinction from the standard value of  $\langle E \rangle_{LMC} = 0.1$  to  $\gtrsim 0.2$ , as first suggested by Freedman et al. (1992) to solve the negative extinction estimates in NGC 300 and recently reintroduced by Böhm-Vitense (1997) in an analysis of the Galactic, LMC, SMC, and M31 Cepheids. In our larger sample and after including the scatter in the extinction, we find the problem is significantly worse and that a mean LMC extinction of  $\gtrsim 0.25$  would be required to eliminate the problem completely. However, even the high estimates of the mean extinction in the LMC by Bessel (1991) based on polarization, HI column density, interstellar absorption lines, and intrinsic color estimates correspond only to  $\langle E \rangle_{LMC} \simeq 0.13$ , and 90% of the LMC supergiants studied by Grieve & Madore (1986) had extinctions less than 0.18, so simply raising the mean LMC extinction is an implausible solution to the problem of negative extinctions. If we can reject raising the LMC extinction, then the need for negative extinctions is conclusive evidence for adding additional physics to the Cepheid model or for substantial correlated systematic errors in the magnitudes beyond the simple HST calibration uncertainties.

The physical requirement that the extinction be positive also means that the standard Cepheid distance estimates are systematically biased by their equal treatment of positive and negative extinctions. The covariance of distance and extinction mean that low extinction estimates are associated with higher distances, so any requirement for positivity in the extinction will drive the distances to all Cepheid galaxies downwards. The bias extends equally to galaxies with and without a negative extinction problem because the



extinction estimates and distances are also correlated between galaxies – if I force a reduction in the distance to one galaxy, the correlations lead to a reduction in the distances to all galaxies.

A partial solution to the negative extinction problem is to use a finite temperature distribution at fixed period so that blue Cepheids are interpreted as being hotter rather than having lower extinctions (see the discussion in Freedman et al. 1992). It is only a partial solution both because the instability strip is narrow and because it cannot significantly change the mean extinction of the distribution unless there are few Cepheids in the galaxy. In Model 2 we allowed the Cepheids a temperature distribution, and forced the positivity of the extinction for a range of LMC mean extinctions. As expected from the bias in the standard distance estimates, the distance to every Cepheid galaxy decreased by mean values of  $-0.20$ ,  $-0.14$ , and  $-0.05$  mag for LMC mean extinctions of  $\langle E \rangle_{LMC} = 0.10$ ,  $0.15$ , and  $0.20$  respectively. All Hubble constant estimates systematically rise, although the effect is more dramatic for the low metallicity Type Ia Project galaxies because of their bluer Cepheids. In particular, the MLCS Hubble constant estimates become  $80 \pm 6$ ,  $78 \pm 6$  and  $72 \pm 6$  km s $^{-1}$  Mpc $^{-1}$  and the M100 (Mould et al. 1995) estimates become  $90$ ,  $88$ , and  $84$  km s $^{-1}$  Mpc $^{-1}$  in order of increasing LMC extinction. Model 2 is only a partial solution to the negative extinction problem, and despite the addition of a temperature variable for all 694 Cepheids, the likelihood of the solutions declined significantly compared to Model 1.

The extinctions shows a rough correlation with the metallicity of the host galaxy, as would be expected from theoretical models predicting that metal poor Cepheids should be bluer than metal rich Cepheids (e.g. Stothers (1988), Stif (1990, 1995), Chiosi et al. 1993). In Model 3 we added a metallicity correction to the Cepheid zero-point, similar to the model of Sasselov et al. (1996), and we find a change in the mean V and I magnitude of  $-0.14 \pm 0.14$  mag/dex and a change in the V–I color of  $0.13 \pm 0.04$  mag/dex. The metallicity

terms change little with the assumptions about the LMC extinction. The trend with wavelength is that metal rich Cepheids become fainter in U and B, start getting brighter at V, and show the largest increases in the infrared, as expected from line-blanketing increasing the opacity towards the blue and back-warming increasing the emission towards the red. While the quantitative estimates may be somewhat high, they roughly agree with both the theoretical expectations and other experimental or semi-empirical determinations (e.g. Caldwell & Coulson 1986, 1987, Gieren et al. 1993, Stiff 1995, Sasselov et al. 1996). The change in color with metallicity is more important than the change in luminosity, so studies focusing only on the change in luminosity (Madore & Freedman 1990, Gould 1994) miss the dominant effect. The addition of the metallicity correction lets the model solve the negative extinction problems without simply driving the distance estimates downwards, and as discussed in Gould (1994) and Sasselov et al. (1996), it can also explain many of the discrepancies between low (Type Ia supernovae in low metallicity galaxies) and high (other distance indicators in high metallicity galaxies) estimates of the Hubble constant. The MLCS Hubble constant estimates from the low metallicity galaxies are  $85 \pm 6$ ,  $80 \pm 6$  and  $76 \pm 6$  km s<sup>-1</sup> Mpc<sup>-1</sup>, while the high metallicity M100 estimates are 83, 78 and 74 km s<sup>-1</sup> Mpc<sup>-1</sup> as we increase the mean LMC extinction. A metallicity dependence to the Cepheid distance scale is the most plausible explanation of the negative extinction problem if it cannot be explained by systematic errors in the photometry. Otherwise, the qualitative effect is probably secure even if our quantitative results are changed by improved data or metallicity estimates

There is no question that the models including temperature and metallicity are beginning to push the limits of the data, although our inclusion of the covariances between variables should properly treat near degeneracies. We can identify five areas for improvement in the data. The first is that the data on the LMC Cepheids needs to be expanded and observed in a more uniform set of filters. The enormous MACHO and EROS

samples of Cepheids can almost fill this role, but the calibration uncertainties need to be reduced, comparisons to standard filters need to be better understood, and comparable data in additional filters is required. The second problem is that the HST Cepheid samples have only two-color photometry. Since even the simplest models that can fully probe the systematic uncertainties in the Cepheid distance scale require extinction, temperature and composition estimates for each individual Cepheid, a minimum of four-color photometry is needed. The two additional filters should be B (sensitive to extinction and metallicity) and H or K (sensitive to temperature and metallicity). *Without additional colors it will be difficult or impossible to cleanly address the systematic problems in the Cepheid distance scale.* The third problem is that the formal uncertainties in the absolute calibration of the HST magnitudes (about 0.05 mag) are large compared to the effects we are probing. Some means of improving the absolute calibrations is critical to better controlling the systematic uncertainties in the Cepheid distance scale. The fourth problem is that many of the Cepheid host galaxies lack metallicity measurements, forcing us to rely on general correlations between galaxy type or luminosity and metallicity.

The final problem is that no matter how elaborate or rococo we make the analysis procedures for Cepheid mean magnitudes, it is not the proper way to analyze the data. The only “correct” way to analyze the Cepheid data is to directly fit the observed light curves, in the spirit of the MLCS method for Type Ia supernovae (Riess et al. 1995). Such an approach is critical to the extragalactic samples where heroic investments of HST time still produce poor phase coverage in V and terrible phase coverage in I, let alone adding data in the two additional filters needed to control systematic uncertainties. Stetson (1996) has developed a template method for identifying Cepheids and better estimating mean magnitudes, and in our second paper on Cepheid distances (Kochanek 1997) we develop an improved template method incorporating both color and velocity data. Ideally, the shapes of the light curves also constrain the gross physical properties of the Cepheids and

break some of the close degeneracies seen between temperature, extinction, distance, and metallicity that limit the validity and accuracy of our current conclusions.

Acknowledgements: I would like to thank many people for material and intellectual help, particularly J.A.R. Caldwell, N.R. Evans, W.L. Freedman, J. Huchra, M. Krockenberger and D. Sasselov. R. Kirshner, R. Kurucz, A. Saha and D. Welch offered helpful comments. J.A.R. Caldwell provided his latest compilation of phase-averaged data on the LMC and SMC Cepheids, and W.L. Freedman and A. Gould helped reconstruct the unpublished M31 data.

## REFERENCES

- Backer, D.C., 1996, in *Unsolved Problems of the Milky Way*, eds. L. Blitz & P. Teuben  
(Kluwer Acad. Publ.: Dordrecht) 193
- Beaulieu, J.P., Grison, P., Tobin, W., et al., 1995, *A&A*, 303, 137
- Berdnikov, L.N., 1987, *PZ*, 22, 505
- Berdnikov, L.N., 1996, <http://www.sai.msu.su/groups/cluster/cepheids>
- Bessel, M.S., 1991, *A&A*, 242, L17
- Blair, W.P., Kirshner, R.P., & Chevalier, R.A., 1982, *ApJ*, 254, 50
- Böhm-Vitense, E., 1997, *AJ*, 113, 13
- Burstein, D., & Heiles, C., 1984, *ApJS*, 54 33
- Caldwell, J.A.R., 1996, private communication
- Caldwell, J.A.R., & Coulson, I.M., 1986, *MNRAS*, 218, 223
- Caldwell, J.A.R., & Coulson, I.M., 1987, *AJ*, 93, 1090
- Caldwell, J.A.R., & Laney, C.D., 1991, in *The Magellanic Clouds*, eds., R. Haynes & D.  
Milne, (Kluwer: Dordrecht) 249
- Cardelli, J.A., Clayton, G.C., & Mathis, J.S., 1989, *ApJ*, 345, 245
- Ciardullo, R., Jacoby, G.H., & Tonry, J.L., 1993, *ApJ*, 419, 479
- Chiosi, C., Wood, P.R., & Capitanio, N., 1993, *ApJS*, 86, 541
- Dennefeld, M., & Knuth, D., 1981, *AJ*, 86, 989

- Eastman, R.G., Schmidt, B.G., & Kirshner, R., 1996, *ApJ*, 466, 911
- Feast, M.W., & Walker, A.R., 1987, *ARA&A*, 25, 345
- Fernie, J.D., 1990, *ApJ*, 354, 295
- Fernie, J.D., Beattie, B., Evans, N.R., & Seager, S., 1995, *IBVS*, 4148
- Ferrarese, L., Freedman, W.F., Hill, R.J., et al., 1996, *ApJ*, 464, 568
- Ferrarese, L., Freedman, W.F., Hill, R.J., et al., 1997, *ApJ*, 475, 853
- Freedman, W.L., 1985, in *Cepheids: Theory & Observations*, IAU Colloquium 82, ed. B.F. Madore (Cambridge: Cambridge University Press) 225
- Freedman, W.L., & Madore, B.F., 1990, *ApJ*, 365, 186
- Freedman, W.L., Wilson, C.D., & Madore, B.F., 1991, *ApJ*, 372, 455
- Freedman, W.L., Madore, B.F., Hawley, S.L., Horowitz, I.K., Mould, J., Navarrete, M., & Sallman, S., 1992, *ApJ*, 396, 80
- Freedman, W.L., Hughes, S.M., Madore, B.F., et al., 1994, *ApJ*, 427, 628
- Freedman, W.L., 1996, private communication
- Freedman, W.L., 1997, in *Critical Dialogues in Cosmology*, astro-ph/9612024
- Gould, A., 1994, *ApJ*, 426, 542
- Graham, J.A., Phelps, R.L., & Freedman, W.L., et al., 1996, preprint
- Grieve, G.R., & Madore, B.F., 1986, *ApJS*, 62, 451
- Höflich, P., & Khokhlov, A., 1996, *ApJ*, 457, 500

- Hughes, S.M., Stetson, P.B., Turner, A., et al., 1994, *ApJ*, 428, 143
- Huterer, D., Sasselov, D.D., & Schechter, P.L., 1995, *AJ*, 110, 2705
- Jacoby, G.H., Walker, A.R., & Ciardullo, R., 1990, *ApJ*, 365, 471
- Kelson, D.D., Illingworth, G.D., Freedman, W.F., et al., 1996, *ApJ*, 463, 26
- Laney, C.D., & Stobie, R.S., 1986, *MNRAS*, 222, 449
- Laney, C.D., & Stobie, R.S., 1993, *MNRAS*, 263, 921
- Laney, C.D., & Stobie, R.S., 1994, *MNRAS*, 266, 411
- Lin, D.N.C., & Lynden-Bell, D., 1982, *MNRAS*, 198, 707
- Madore, B.F., 1985, in *Cepheids: Theory & Observations*, ed. B.F. Madore (Cambridge Univ. Press: Cambridge) 166
- Madore, B.F., McAlary, C.W., McLaren, R.A., Welch, D.L., & Neugebauer, G., 1985, *ApJ*, 294, 560
- Madore, B.F., & Freedman, W.F., 1991, *PASP*, 103, 933
- Oey, M.S., & Kennicutt, R.C., 1993, *ApJ*, 411, 137
- Pont, F., Burki, G., & Mayor, G., 1994, *A&A*, 285, 415
- Reid, M.J., 1993, *ARA&A*, 31, 1993
- Riess, A.G., Press, W.H., & Kirshner, R.P., 1995, *ApJL*, 438, L17
- Riess, A.G., Press, W.H., & Kirshner, R.P., 1996, *ApJ*, 473, 88
- Saha, A., Labhardt, L., Schwengeler, H., Macchetto, F.D., Panagia, N., Sandage, A., & Tammann, G.A., 1994, *ApJ*, 425, 14

- Saha, A., Sandage, A., Labhardt, L., Schwengeler, H., Tammann, G.A., Panagia, N., & Macchetto, F.D., 1995, ApJ, 438, 8
- Saha, A., Sandage, A., Labhardt, L., Tammann, G.A., Macchetto, F.D., Panagia, N., 1996, ApJ, 466, 55
- Saha, A., Sandage, A., Labhardt, L., Tammann, G.A., Macchetto, F.D., Panagia, N., 1996, ApJS in press
- Saha, A., Sandage, A., Labhardt, L., Tammann, G.A., Macchetto, F.D., Panagia, N., 1997, Carnegie Institution Preprint
- Sasselov, D.D., Beaulieu, J.P., Renault, C., et al., 1996, A&A in press
- Schechter, P.L., Avruch, I.M., Caldwell, J.A.R., & Keane, M.J., 1992, AJ, 104, 1930
- Silbermann, N.A., Harding, P., Madore, B.F., et al., 1996, ApJ in press
- Stetson, P.B., 1996, PASP, 108, 851
- Stift, M.J., 1990, A&A, 229, 143
- Stift, M.J., 1995, A&A, 301, 776
- Stothers, R.B., 1988, ApJ, 329, 712
- Tanvir, N.R., Shanks, T., Ferguson, H.C., & Robinson, D.R.T., 1995, Nature, 377, 27
- Tanvir, N.R., 1996, The Extragalactic Distance Scale, astro-ph/9611027
- Tonry, J.L., Blakeslee, J.P., Ajhar, E.A., & Dressler, A., 1996, astro-ph/9609113
- Welch, D.L., McLaren, R.A., Madore, B.F., & McAlarney, C.W., 1987, ApJ, 321, 162
- Welch, D.L., 1996, <http://www.physics.mcmaster.ca/Cepheid/HomePage.html>



Welch, D.L., et al., 1997, astro-ph/9610024

Westerlund, B.E., 1990, A&AR, 2, 29

Zaritsky, D., Kennicutt, R.C., & Huchra, J.P., 1994, ApJ, 420, 87

Table 1. Cepheid Data

Galaxy	Group	$N_i$	Bands	$E_f$	$[O/H]$
Galaxy		124	UBVRIJHK	–	0.30
LMC		71	UBVRIJHK	0.063	0.00
SMC		78	UBVRIJHK	0.043	–0.35
M 33	Local	11	BVRI	0.045	$0.58 \pm 0.04$
M 31	Local	30	BVRI	0.080	$0.28 \pm 0.27$
NGC 300	Sculptor	13	BVRI	0.025	$0.05 \pm 0.15$
M 81	M 81	31	VI	0.038	$0.32 \pm 0.07$
M 101	M 101	29	VI	–0.008	$0.02 \pm 0.00$
IC 4182		19	VI	–0.015	–0.35
NGC 5253	Centaurus	8	VI	0.048	–0.25
NGC 925	NGC 1023	73	VI	0.065	$0.29 \pm 0.02$
M 96	Leo I	7	VI	0.015	0.69
NGC 3351	Leo I	46	VI	0.013	$0.94 \pm 0.03$
NGC 4536	Virgo	32	VI	–0.005	0.00
M 100	Virgo	51	VI	0.010	$0.84 \pm 0.04$
NGC 4496A	Virgo	56	VI	0.003	0.00
NGC 4639	Virgo	14	VI	0.013	0.10

Note. — The metallicities are from Zaritsky et al. (1994), except for M 96 (Oey & Kennicutt 1993) and M 31 (Blair et al. 1982). Metallicities for the galaxies not included in Zaritsky et al. (1994) were estimated from the metallicity-type or metallicity-magnitude relations. The metallicity uncertainties represent the rms range of metallicities assigned to the Cepheids in that galaxy based on the metallicity gradients if known. The foreground extinction estimates  $E_f = E(B - V)_f$  are from Burstein & Heiles (1984).

Table 2. Cepheid Correlations

Model	$-2 \ln L$	Vector	U	B	V	R	I	J	H	K
MF1	—	$V_k$		$14.03 \pm 0.08$	$13.24 \pm 0.07$	$12.80 \pm 0.05$	$12.41 \pm 0.04$			
		$\alpha'_k$		$-2.43 \pm 0.14$	$-2.76 \pm 0.11$	$-2.94 \pm 0.09$	$-3.06 \pm 0.07$			
		$\sigma_{PLCk}$		0.36	0.27	0.22	0.18			
MF2	—	$V_k$		$14.03 \pm 0.16$	$13.23 \pm 0.12$	$12.80 \pm 0.11$	$12.40 \pm 0.09$	$11.89 \pm 0.07$	$11.50 \pm 0.06$	$11.43 \pm 0.05$
		$\alpha'_k$		$-2.53 \pm 0.28$	$-2.88 \pm 0.20$	$-3.04 \pm 0.17$	$-3.14 \pm 0.17$	$-3.31 \pm 0.11$	$-3.37 \pm 0.10$	$-3.42 \pm 0.09$
		$\sigma_{PLCk}$		0.40	0.29	0.25	0.21	0.16	0.14	0.13
0	4277	$V_k$	$14.54 \pm 0.05$	$14.05 \pm 0.03$	$13.28 \pm 0.03$	$12.83 \pm 0.03$	$12.45 \pm 0.03$	$11.89 \pm 0.02$	$11.53 \pm 0.02$	$11.45 \pm 0.02$
		$\alpha'_k$	$-2.06 \pm 0.14$	$-2.30 \pm 0.08$	$-2.62 \pm 0.05$	$-2.81 \pm 0.06$	$-2.95 \pm 0.05$	$-3.22 \pm 0.05$	$-3.31 \pm 0.05$	$-3.35 \pm 0.04$
		$R_k$	$5.20 \pm 0.08$	$4.30 \pm 0.06$	$\equiv 3.3$	$2.66 \pm 0.05$	$2.02 \pm 0.05$	$1.05 \pm 0.06$	$0.66 \pm 0.06$	$0.47 \pm 0.06$
		$\sigma_{PLCk}$	$0.27 \pm 0.02$	$0.29 \pm 0.01$	$0.27 \pm 0.01$	$0.15 \pm 0.01$	$0.21 \pm 0.01$	$0.13 \pm 0.01$	$0.11 \pm 0.01$	$0.10 \pm 0.01$
1	7418	$V_k$	$14.60 \pm 0.02$	$14.06 \pm 0.01$	$13.29 \pm 0.01$	$12.86 \pm 0.01$	$12.44 \pm 0.01$	$11.86 \pm 0.01$	$11.49 \pm 0.01$	$11.41 \pm 0.01$
		$\alpha'_k$	$-1.83 \pm 0.12$	$-2.25 \pm 0.05$	$-2.63 \pm 0.07$	$-2.79 \pm 0.03$	$-2.95 \pm 0.04$	$-3.16 \pm 0.03$	$-3.26 \pm 0.03$	$-3.30 \pm 0.03$
		$R_k$	$5.13 \pm 0.04$	$4.28 \pm 0.02$	$\equiv 3.3$	$2.72 \pm 0.01$	$2.17 \pm 0.02$	$1.31 \pm 0.03$	$0.95 \pm 0.03$	$0.78 \pm 0.03$
		$\sigma_{PLCk}$	$0.03 \pm 0.03$	$0.00 \pm 0.01$	$0.00 \pm 0.01$	$0.00 \pm 0.01$	$0.02 \pm 0.01$	$0.06 \pm 0.01$	$0.06 \pm 0.01$	$0.07 \pm 0.01$
2-15	7340	$V_k$	$14.34 \pm 0.03$	$13.82 \pm 0.02$	$13.13 \pm 0.02$	$12.75 \pm 0.02$	$12.38 \pm 0.02$	$11.87 \pm 0.02$	$11.53 \pm 0.02$	$11.46 \pm 0.02$
		$\alpha'_k$	$-1.95 \pm 0.12$	$-2.31 \pm 0.09$	$-2.67 \pm 0.07$	$-2.80 \pm 0.06$	$-2.96 \pm 0.05$	$-3.15 \pm 0.04$	$-3.25 \pm 0.03$	$-3.29 \pm 0.03$
		$R_k$	$5.37 \pm 0.05$	$4.45 \pm 0.02$	$\equiv 3.3$	$2.60 \pm 0.02$	$1.95 \pm 0.03$	$0.95 \pm 0.04$	$0.51 \pm 0.05$	$0.32 \pm 0.05$
		$\beta_k$	$-1.86 \pm 0.04$	$-1.23 \pm 0.03$	$\equiv -1.00$	$-0.89 \pm 0.02$	$-0.87 \pm 0.02$	$-0.70 \pm 0.02$	$-0.61 \pm 0.03$	$-0.58 \pm 0.03$
3-15	7270	$V_k$	$14.36 \pm 0.03$	$13.84 \pm 0.02$	$13.02 \pm 0.02$	$12.74 \pm 0.02$	$12.36 \pm 0.02$	$11.88 \pm 0.02$	$11.53 \pm 0.02$	$11.46 \pm 0.02$
		$\alpha'_k$	$-1.86 \pm 0.12$	$-2.28 \pm 0.09$	$-2.66 \pm 0.07$	$-2.81 \pm 0.06$	$-2.97 \pm 0.05$	$-3.15 \pm 0.04$	$-3.26 \pm 0.04$	$-3.30 \pm 0.04$
		$R_k$	$5.23 \pm 0.06$	$4.33 \pm 0.03$	$\equiv 3.3$	$2.62 \pm 0.02$	$2.00 \pm 0.03$	$0.89 \pm 0.05$	$0.51 \pm 0.06$	$0.32 \pm 0.06$
		$\beta_k$	$-1.86 \pm 0.05$	$-1.25 \pm 0.03$	$\equiv -1.00$	$-0.87 \pm 0.03$	$-0.86 \pm 0.02$	$-0.68 \pm 0.03$	$-0.60 \pm 0.03$	$0.57 \pm 0.03$
		$\gamma'_k$	$0.34 \pm 0.22$	$0.20 \pm 0.18$	$-0.08 \pm 0.14$	$-0.18 \pm 0.14$	$-0.21 \pm 0.14$	$-0.26 \pm 0.13$	$-0.34 \pm 0.14$	$-0.40 \pm 0.13$
Priors		$R_k$	$5.05 \pm 0.10$	$4.31 \pm 0.10$	$\equiv 3.3$	$2.73 \pm 0.10$	$2.07 \pm 0.10$	$0.95 \pm 0.10$	$0.64 \pm 0.10$	$0.39 \pm 0.10$
		$\beta_k$	$-1.84 \pm 0.05$	$-1.40 \pm 0.05$	$\equiv -1.00$	$-0.84 \pm 0.05$	$-0.70 \pm 0.05$	$-0.52 \pm 0.05$	$-0.38 \pm 0.05$	$0.36 \pm 0.05$

Note. — All correlations assume an LMC distance modulus of 18.5 mag. The mean LMC extinction is  $E(B - V) = 0.10$  for MF1, MF2, Model 0, and Model 1, and it is  $E(B - V) = 0.15$  for Models 2-15 and 3-15. MF1 and MF2 are the Madore & Freedman (1991) PLC relations for the LMC after shifting the period origin to  $\log P_0 = 1.4$  from 1.0. The uncertainties in MF1 and MF2 the zero-points may be exaggerated by the shift in the period origin because we did not possess the correlations in the  $V_k - \alpha'_k$  errors.

Table 3. Cepheid Distances & Extinctions

Galaxy	Var	Published	Model 0	Model 1	Model 2–15	Model 3–15
Galaxy	$R_0$	$14.52 \pm 0.15$	$14.37 \pm 0.17$	$14.12 \pm 0.11$	$14.42 \pm 0.11$	$14.53 \pm 0.12$
	$\Theta_0(\text{ km s}^{-1})$	$254 \pm 21$	$244 \pm 18$	$240 \pm 13$	$241 \pm 14$	$241 \pm 14$
LMC	$\mu - \mu_{LMC}$		$\equiv 0.00$	$\equiv 0.0$	$\equiv 0.0$	$\equiv 0.0$
	$\langle E(B - V) \rangle$	0.08	$\equiv 0.10$	$\equiv 0.10$	$\equiv 0.15$	$\equiv 0.15$
	$\sigma_E$	0.03		$0.095 \pm 0.006$	$0.079 \pm 0.007$	$0.079 \pm 0.007$
SMC	$\mu - \mu_{LMC}$	$0.4 \pm 0.1$	$0.47 \pm 0.02$	$0.53 \pm 0.02$	$0.48 \pm 0.02$	$0.33 \pm 0.05$
	$\langle E(B - V) \rangle$	0.04	$0.052 \pm 0.010$	$0.037 \pm 0.003$	$0.100 \pm 0.003$	$0.137 \pm 0.014$
	$\sigma_E$	0.02		$0.082 \pm 0.004$	$0.066 \pm 0.005$	$0.066 \pm 0.005$
M 33	$\mu - \mu_{LMC}$	$6.14 \pm 0.09$	$6.02 \pm 0.15$	$6.00 \pm 0.06$	$6.00 \pm 0.05$	$6.35 \pm 0.09$
	$\langle E(B - V) \rangle$	$0.10 \pm 0.09$	$0.161 \pm 0.050$	$0.162 \pm 0.020$	$0.209 \pm 0.016$	$0.107 \pm 0.030$
	$\sigma_E$			$0.055 \pm 0.013$	$0.012 \pm 0.050$	$0.010 \pm 0.050$
M 31	$\mu - \mu_{LMC}$	$5.94 \pm 0.14$	$5.83 \pm 0.10$	$5.77 \pm 0.04$	$5.80 \pm 0.03$	$5.97 \pm 0.05$
	$\langle E(B - V) \rangle$	$0.19 \pm 0.13$	$0.194 \pm 0.032$	$0.211 \pm 0.012$	$0.249 \pm 0.010$	$0.200 \pm 0.015$
	$\sigma_E$			$0.106 \pm 0.012$	$0.110 \pm 0.016$	$0.105 \pm 0.019$
NGC 300	$\mu - \mu_{LMC}$	$8.16 \pm 0.10$	$8.11 \pm 0.14$	$8.13 \pm 0.03$	$8.02 \pm 0.03$	dropped
	$\langle E(B - V) \rangle$	$-0.07 \pm 0.03$	$-0.037 \pm 0.047$	$-0.048 \pm 0.010$	$0.034 \pm 0.008$	
	$\sigma_E$			$0.052 \pm 0.009$	$0.055 \pm 0.016$	
M 81	$\mu - \mu_{LMC}$	$9.30 \pm 0.20$	$9.22 \pm 0.21$	$9.22 \pm 0.09$	$9.05 \pm 0.09$	$9.13 \pm 0.11$
	$\langle E(B - V) \rangle$	$0.03 \pm 0.05$	$0.075 \pm 0.076$	$0.071 \pm 0.027$	$0.180 \pm 0.037$	$0.183 \pm 0.036$
	$\sigma_E$			$0.095 \pm 0.012$	$0.072 \pm 0.018$	$0.065 \pm 0.017$
M 101	$\mu - \mu_{LMC}$	$10.84 \pm 0.17$	$10.82 \pm 0.21$	$10.84 \pm 0.11$	$10.66 \pm 0.09$	$10.56 \pm 0.11$
	$\langle E(B - V) \rangle$	$0.03 \pm ??$	$0.015 \pm 0.079$	$0.009 \pm 0.024$	$0.123 \pm 0.033$	$0.166 \pm 0.044$
	$\sigma_E$			$0.095 \pm 0.010$	$0.079 \pm 0.015$	$0.079 \pm 0.017$
IC 4182	$\mu - \mu_{LMC}$	$9.86 \pm 0.09$	$9.98 \pm 0.23$	$10.05 \pm 0.08$	$9.81 \pm 0.11$	$9.57 \pm 0.14$
	$\langle E(B - V) \rangle$	$-0.08 \pm 0.07$	$-0.041 \pm 0.076$	$-0.064 \pm 0.031$	$0.065 \pm 0.039$	$0.153 \pm 0.056$
	$\sigma_E$			$0.081 \pm 0.013$	$0.044 \pm 0.022$	$0.044 \pm 0.023$
NGC 5253	$\mu - \mu_{LMC}$	$9.58 \pm 0.10$	$9.20 \pm 0.32$	$9.23 \pm 0.16$	$9.07 \pm 0.13$	$8.90 \pm 0.15$
	$\langle E(B - V) \rangle$	$0.02 \pm 0.29$	$0.071 \pm 0.125$	$0.058 \pm 0.061$	$0.165 \pm 0.046$	$0.209 \pm 0.051$
	$\sigma_E$			$0.080 \pm 0.023$	$0.044 \pm 0.038$	$0.054 \pm 0.032$
NGC 925	$\mu - \mu_{LMC}$	$11.34 \pm 0.16$	$11.33 \pm 0.18$	$11.31 \pm 0.08$	$11.18 \pm 0.10$	$11.23 \pm 0.10$
	$\langle E(B - V) \rangle$	$0.13 \pm 0.08$	$0.136 \pm 0.067$	$0.137 \pm 0.035$	$0.235 \pm 0.031$	$0.244 \pm 0.034$
	$\sigma_E$			$0.102 \pm 0.007$	$0.069 \pm 0.010$	$0.069 \pm 0.011$
M 96	$\mu - \mu_{LMC}$	$11.82 \pm 0.16$	$11.78 \pm 0.28$	$11.83 \pm 0.10$	$11.64 \pm 0.10$	$11.92 \pm 0.15$
	$\langle E(B - V) \rangle$	$0.06 \pm 0.03$	$0.061 \pm 0.117$	$0.043 \pm 0.029$	$0.159 \pm 0.043$	$0.127 \pm 0.038$
	$\sigma_E$			$0.093 \pm 0.023$	$0.076 \pm 0.029$	$0.067 \pm 0.030$

Table 3—Continued

Galaxy	Var	Published	Model 0	Model 1	Model 2–15	Model 3–15
NGC 3351	$\mu - \mu_{LMC}$	$11.51 \pm 0.19$	$11.42 \pm 0.19$	$11.41 \pm 0.06$	$11.27 \pm 0.08$	$11.59 \pm 0.14$
	$\langle E(B - V) \rangle$	$0.12 \pm 0.02$	$0.122 \pm 0.073$	$0.122 \pm 0.047$	$0.222 \pm 0.033$	$0.176 \pm 0.032$
	$\sigma_E$			$0.122 \pm 0.013$	$0.105 \pm 0.014$	$0.104 \pm 0.014$
NGC 4536	$\mu - \mu_{LMC}$	$12.60 \pm 0.13$	$12.47 \pm 0.22$	$12.35 \pm 0.11$	$12.22 \pm 0.09$	$12.11 \pm 0.12$
	$\langle E(B - V) \rangle$	$0.04 \pm 0.04$	$0.077 \pm 0.079$	$0.117 \pm 0.032$	$0.215 \pm 0.035$	$0.261 \pm 0.042$
	$\sigma_E$			$0.083 \pm 0.011$	$0.065 \pm 0.015$	$0.064 \pm 0.015$
M 100	$\mu - \mu_{LMC}$	$12.54 \pm 0.17$	$12.49 \pm 0.20$	$12.50 \pm 0.10$	$12.32 \pm 0.09$	$12.60 \pm 0.15$
	$\langle E(B - V) \rangle$	$0.10 \pm 0.06$	$0.075 \pm 0.072$	$0.071 \pm 0.020$	$0.182 \pm 0.031$	$0.143 \pm 0.029$
	$\sigma_E$			$0.117 \pm 0.011$	$0.098 \pm 0.012$	$0.097 \pm 0.012$
NGC 4496A	$\mu - \mu_{LMC}$	$12.53 \pm 0.14$	$12.41 \pm 0.20$	$12.43 \pm 0.11$	$12.27 \pm 0.10$	$12.17 \pm 0.13$
	$\langle E(B - V) \rangle$	$0.03 \pm 0.04$	$0.061 \pm 0.074$	$0.056 \pm 0.028$	$0.162 \pm 0.037$	$0.207 \pm 0.044$
	$\sigma_E$			$0.094 \pm 0.008$	$0.066 \pm 0.011$	$0.066 \pm 0.011$
NGC 4639	$\mu - \mu_{LMC}$	$13.53 \pm 0.22$	$13.61 \pm 0.32$	$13.59 \pm 0.21$	$13.24 \pm 0.11$	$13.28 \pm 0.13$
	$\langle E(B - V) \rangle$	$?? \pm ??$	$-0.083 \pm 0.114$	$-0.078 \pm 0.072$	$0.091 \pm 0.035$	$0.093 \pm 0.039$
	$\sigma_E$			$0.112 \pm 0.021$	$0.097 \pm 0.030$	$0.098 \pm 0.031$

Note. — The published extinction estimates for M 33, M 31, IC 4182, NGC 5253, NGC 4536, NGC 4496A, and NGC 4639 are not directly comparable to our estimates because the authors used different extinction models. A ? indicates that no estimate was included in the published results. The value for the solar radius  $R_0$  is the consensus value from Reid (1993), and the value for the circular velocity of the sun  $\Theta_0$  combines the  $R_0$  estimate with the proper motion of Sgr A\* (Backer 1996). The relative distance of the LMC and the SMC and the extinction values are from the review by Westerlund (1990), although Jacoby et al. (1990) find higher values of 0.13 for the LMC and 0.06 for the SMC based on Balmer decrements in planetary nebulae. Our distances and the Westerlund (1990) value for the SMC are larger than the Caldwell & Laney (1991) values because of differences in defining the Cloud centers. **The distance errors are very strongly correlated and cannot be treated as independent, random uncertainties!**

Table 4. Comparison Distances

Galaxy	EPM	SNIa	SBF	SNIa/MLCS
	$\mu - 18.5$	$\mu - 18.5$	$\mu - \mu_{M31}$	$\mu - \mu_{SN1981B}$
M 31			$\equiv 0 \pm 0.06$	
M 81			$3.26 \pm 0.08$	
M 101	$10.85^{+0.28}_{-0.49}$			
IC 4182		$9.77^{+0.44}_{-0.55}$		
NGC 5253	$(9.56 \pm 0.2)$	$9.51^{+0.30}_{-0.35}$	$3.65 \pm 0.10$	$-3.17 \pm 0.09$
NGC 925	$(11.63^{+0.35}_{-0.24})$		$5.53 \pm 0.09$	
M 96	$(12.38^{+0.93}_{-1.37})$		$(5.76 \pm 0.06)$	
NGC 3351	$(12.38^{+0.93}_{-1.37})$		$(5.76 \pm 0.06)$	
NGC 4536		$12.89^{+0.41}_{-0.51}$		$\equiv 0 \pm 0.07$
M 100	$12.37^{+0.51}_{-0.67}$			
NGC 4639	$13.00^{+0.48}_{-0.62}$			$0.66 \pm 0.14$

Note. — Absolute distances for the Cepheid galaxies based on the expanding photosphere method (EPM, Eastman, Schmidt & Kirshner 1996) or physical models of Type Ia supernovae (SNIa, Höflich & Khokhlov 1996), and relative distances based on the surface brightness fluctuation method (SBF, Tonry et al. 1996) and the MLCS method for Type Ia supernovae (SNIa/MLCS, Riess et al. 1996). The SBF distances are relative to M31, and the MLCS distances are relative to SN 1981B in NGC 4536. Values without parenthesis are distances to the Cepheid galaxy, while values in parenthesis are for galaxies in the same group.